

# Randomized Matrix Decompositions using R

**N. Benjamin Erichson**  
University of St Andrews

**Sergey Voronin**  
Tufts University

**Steven L. Brunton**  
University of Washington

**J. Nathan Kutz**  
University of Washington

---

## Abstract

The singular value decomposition (SVD) is among the most ubiquitous matrix factorizations and is a cornerstone algorithm for data analysis, dimensionality reduction and data compression. However, despite modern computer power, massive data-sets pose a computational challenge for traditional SVD algorithms. We present the R package **rsvd**, which enables the fast computation of the SVD and related methods, facilitated by randomized algorithms. Specifically, the package provides routines for computing the randomized singular value decomposition, randomized principal component analysis and randomized robust principal component analysis. Randomized algorithms provide an efficient computational framework for reducing the computational demands of traditional (deterministic) matrix factorizations. The key idea is to compute a compressed representation of the data using random sampling. This smaller matrix captures the essential information that can then be used to obtain a low-rank matrix approximation. Several numerical examples support this powerful concept and show substantial accelerated computational times.

*Keywords:* randomized singular value decomposition, randomized principal component analysis, robust principal component analysis, randomized subspace learning, R.

---

## 1. Introduction

Advances in sensor technology and data acquisition generate a torrential stream of data. Massive data sets emerge across the social, physical, biological and ecological science, in form of social networks, hyper spectral imagery, DNA microarrays, and animal movement data. This forces a shift from classical statistical data analysis concerned with a moderate size of observations and a few carefully selected and meaningful variables, towards the analysis of massive unstructured data ([Donoho 2000](#)).

Matrix factorizations are the fundamental tools for data processing, used in statistical computing and machine learning. In particular, the singular value decomposition (SVD) is a cornerstone algorithm extensively used for data analysis, dimensionality reduction, and data compression. SVD is the workhorse algorithm behind linear regression, (robust) principal component analysis, discriminant analysis and canonical correlation analysis. However, the emergence of massive data poses a computational challenge for classical deterministic matrix algorithms. Randomized accelerated matrix algorithms provide an efficient computational framework, enabling a substantial reduction of the computational demands ([Mahoney 2011](#)).

These algorithms perform computations on a compressed representation of the original data matrix with only a minor loss in precision. This concept is most interesting because many high-dimensional data exhibit a low-dimensional structure, i.e., the intrinsic rank of the data matrix is much lower than the ambient dimension. Hence, such matrices are highly compressible and the randomized singular value decomposition (rSVD) can substantially ease the computational challenges in obtaining an approximate low-rank singular value decomposition. This enables even the decomposition of massive matrices where traditional deterministic algorithms fail. Further, the randomized SVD algorithm comes with strong theoretical error bounds and the advantage that the error can be controlled by oversampling and subspace iterations.

**Brief overview of the development of the singular value decomposition.** While the origins of the SVD can be traced back to the late 19th century, the field of randomized matrix algorithms is relatively young. Figure 1 shows an incomplete time-line of some major developments of the singular value decomposition. Stewart (1993) gives an excellent historical review of the five mathematicians who developed the fundamentals of the SVD, namely Eugenio Beltrami (1835-1899), Camille Jordan (1838-1921), James Joseph Sylvester (1814-1897), Erhard Schmidt (1876-1959) and Hermann Weyl (1885-1955). The development and fundamentals of modern high-performance algorithms to compute the SVD is related to the seminal work of Golub and Kahan (1965) and Golub and Reinsch (1970).

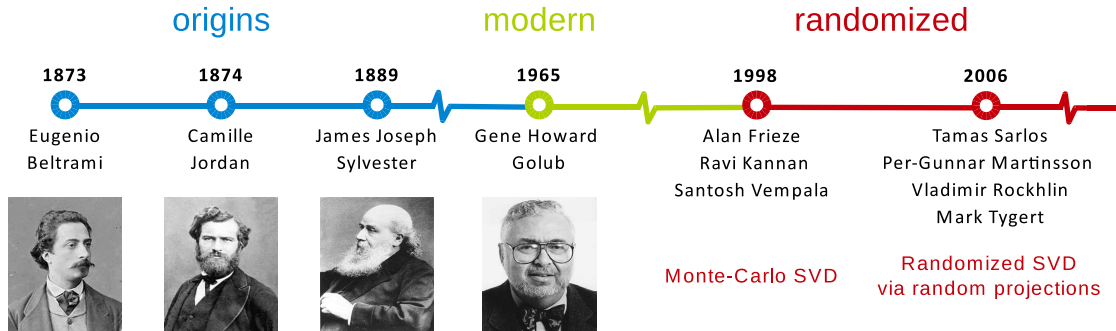


Figure 1: An ‘incomplete’ time-line of major singular value decomposition developments.

The use of randomized matrix algorithms for computing low-rank matrix approximations has become prominent over the past two decades. Frieze, Kannan, and Vempala (2004) introduced the ‘Monte Carlo’ SVD, a rigorous approach to efficiently compute the approximate low-rank SVD based on non-uniform row and column sampling. Sarlos (2006) and Martinsson, Rokhlin, and Tygert (2011) introduced a more robust approach based on random projections. Specifically, the properties of random vectors are exploited to efficiently build a subspace that captures the column space of a matrix. Woolfe, Liberty, Rokhlin, and Tygert (2008) further improved the computational performance by leveraging the properties of highly structured matrices which enable fast matrix multiplications. Eventually, the seminal work by Halko, Martinsson, and Tropp (2011b) unified and expanded the work on the randomized singular value decomposition (rSVD) and introduced state-of-art prototype algorithms to compute the near-optimal low-rank singular value decomposition.

**Motivation and contributions.** The computational costs of the R base SVD algorithm for massive data matrices are tremendous. However, in many applications a near optimal approximation of the low-rank singular value decomposition is sufficient. Specifically, in applications like the principal component analysis, the main interest is in the first few dominant components. Instead of computing the full or truncated SVD using a classic deterministic algorithm, we provide a plug-in function for the more computationally efficient randomized singular value decomposition. Further, we provide functions for computing the principal and robust principal component analysis, facilitated by the randomized SVD algorithm. Specifically, the **rsvd** package provides the following core functions:

- Randomized singular value decomposition: **rsvd()**
- Randomized principal component analysis: **rpca()**
- Randomized robust principal component analysis: **rrpca()**

The interface of the **rsvd()** and **rpca()** functions aims to be as close as possible to the corresponding R base functions. Moreover, the **rpca()** and **rrpca()** allow the user to use a deterministic algorithm instead of the randomized algorithm as well. In addition, several plot functions are provided to visualize the results of the principal component analysis. The package<sup>1</sup> is designed that it can be easily extend and updated.

**Organization.** The remainder of this paper is organized as follows. Following a discussion below on notation, Section 2 briefly reviews the singular value and eigen decompositions and principal component analysis. Section 3 describes the fast randomized algorithm for computing the near optimal low-rank SVD in detail, followed by a discussion of different measurement matrices and a evaluation of the computational performance. This section also discusses the application of randomized methods to eigendecomposition and principal and robust principal component analysis. Section 4 presents motivating examples for using the **rsvd** package, including examples of image compression, eigenfaces, and foreground/background decomposition. Finally, concluding remarks and the roadmap for further developments of the **rsvd** package are presented in Section 5.

**Notation.** By  $\mathbf{A}$ , we denote an  $m \times n$  real valued matrix and by  $\mathbf{A}^T$  the corresponding  $n \times m$  transposed matrix. By  $\|\cdot\|$  we denote the spectral or operator norm, while by  $\|\cdot\|_F$ , we denote the Frobenius norm, where  $\|\mathbf{A}\|_F = \sqrt{\text{trace}(\mathbf{A}^T \mathbf{A})}$ . The relative reconstruction error is computed as  $\|\mathbf{A} - \hat{\mathbf{A}}\|_F / \|\mathbf{A}\|_F$ . We use  $\mathbb{E}[\cdot]$  to denote the expected value and  $\text{VAR}[\cdot]$  to denote the variance of a random variable. By the notation  $D = \text{diag}(a_1, \dots, a_n)$  we refer to an  $n \times n$  diagonal matrix with  $D_{(i,i)} = a_i$ . We express the range (column) space of  $\mathbf{A}$  using  $R(\mathbf{A})$ . By  $\text{trunc}(\mathbf{U}, k)$  we refer to extracting the first or last  $k$  columns of  $\mathbf{U}$  corresponding to the ordering of the singular values, from largest to smallest.

## 2. Matrix decompositions and applications

Here we briefly describe the singular value and eigenvalue decompositions and their application to principal component and robust principal component analysis. The SVD and eigendecomposition are described in great technical detail by Golub and Van Loan (1996), Demmel (1997) and Watkins (2002).

<sup>1</sup>The project page is <https://github.com/Benli11/rSVD>.

## 2.1. Singular value and eigen decompositions.

The singular value decomposition (SVD) is among the most ubiquitous matrix factorizations of the computational era. The SVD is the workhorse algorithm for a wide verity of learning algorithms and data methods. In particular, the SVD provides a numerically stable matrix decomposition that can be used to obtain low-rank approximations, to compute the pseudo-inverses of non-square matrices, and to find the least-squares and minimum norm solutions of a linear model. Given an arbitrary real matrix<sup>2</sup>  $\mathbf{A} \in \mathbb{R}^{m \times n}$ , where  $m \geq n$  without loss of generality, we seek a decomposition, such that

$$\mathbf{A} = \mathbf{U} \mathbf{\Sigma} \mathbf{V}^T \quad (1)$$

as illustrated in Figure 2.

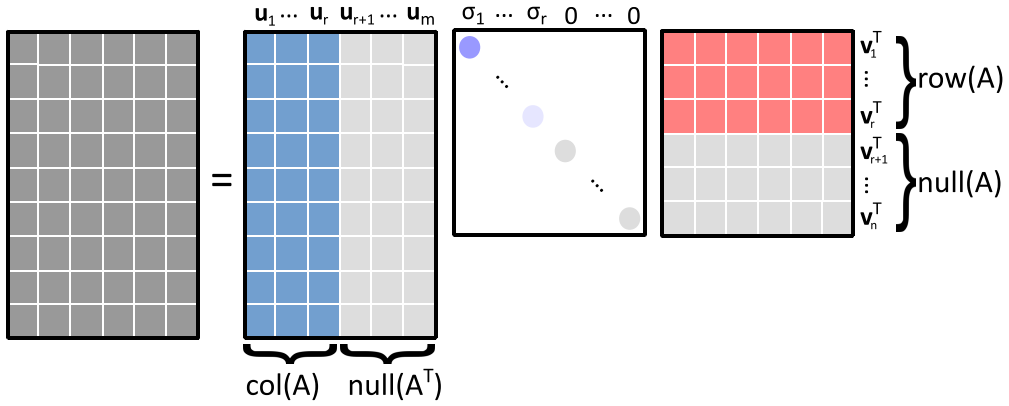


Figure 2: Schematic of the singular value decomposition.

The matrices  $\mathbf{U} = [\mathbf{u}_1, \dots, \mathbf{u}_m] \in \mathbb{R}^{m \times m}$  and  $\mathbf{V} = [\mathbf{v}_1, \dots, \mathbf{v}_n] \in \mathbb{R}^{n \times n}$  are orthonormal so that  $\mathbf{U}^T \mathbf{U} = \mathbf{I}$  and  $\mathbf{V}^T \mathbf{V} = \mathbf{I}$ . The first  $r$  left singular vectors in  $\mathbf{U}$  provide a basis for the range and the first  $r$  right singular vectors in  $\mathbf{V}$  a basis for the domain of the matrix  $\mathbf{A}$ , whereby  $r$  denotes the rank of the data matrix. The rectangular diagonal matrix  $\mathbf{S} \in \mathbb{R}^{m \times n}$  contains the corresponding non-negative singular values  $\sigma_1 \geq \dots \geq \sigma_r$ , describing the spectrum of the data. If the rank  $r$  of the matrix  $\mathbf{X}$  is smaller than the number of columns (i.e.,  $r < n$ ), then the last  $m - r$  singular values  $\{\sigma_i : i \geq r + 1\}$  are zero. The so called ‘economic’ or ‘compact’ SVD computes only the singular vectors corresponding to the non-zero singular values  $\mathbf{U} = [\mathbf{u}_1, \dots, \mathbf{u}_r] \in \mathbb{R}^{m \times r}$  and  $\mathbf{V} = [\mathbf{v}_1, \dots, \mathbf{v}_r] \in \mathbb{R}^{n \times r}$  respectively.

In many cases, the numerical rank  $\bar{r}$  of the matrix is smaller than it’s mathematical rank. That is, many of the last  $\min(m, n) - \bar{r}$  singular values can be close to machine precision. Since the corresponding singular vectors are not in the span of the data, it is often desirable to compute only a reduced version of the SVD. The matrix can be well approximated by including only those eigenvectors which correspond to eigenvalues of a significant amplitude. This number  $k$  can be much smaller than  $\min(m, n)$  depending on the value of  $\bar{r}$ . Choosing an optimal target rank  $k$  is highly dependent on the task, i.e. whether one is interested in a highly accurate reconstruction of the original data or in a very low dimensional representation of dominant features in the data. The low-rank SVD of rank  $k$  takes the form:

$$\mathbf{A}_k = \mathbf{U}_k \mathbf{\Sigma}_k \mathbf{V}_k = [\mathbf{u}_1, \dots, \mathbf{u}_k] \text{diag}(\sigma_1, \dots, \sigma_k) [\mathbf{v}_1, \dots, \mathbf{v}_k]^T. \quad (2)$$

<sup>2</sup>Without loss of generality, the concept applies to complex matrices using the Hermitian transpose instead.

The Eckart-Young theorem (Eckart and Young 1936) establishes that the low-rank SVD provides the optimal rank- $k$  reconstruction of a matrix in the least-square sense, both in the spectral and Frobenius norms:

$$\mathbf{A}_k = \mathbf{U}_k \mathbf{\Sigma}_k \mathbf{V}_k^T := \underset{\mathbf{A}'_k}{\operatorname{argmin}} \|\mathbf{A} - \mathbf{A}'_k\|. \quad (3)$$

Truncating small singular values in the the deterministic SVD gives an optimal approximation of the corresponding rank. The reconstruction error in both the spectral and Frobenius norms is given by:

$$\|\mathbf{A} - \mathbf{A}_k\| = \sigma_{k+1} \quad \text{and} \quad \|\mathbf{A} - \mathbf{A}_k\|_F = \sqrt{\sum_{j=k+1}^{\min(m,n)} \sigma_j^2}. \quad (4)$$

Closely related to the SVD is the eigendecomposition. When  $\mathbf{M}$  is a square  $n \times n$  matrix, we can write  $\mathbf{M} = \mathbf{Q}\mathbf{\Sigma}\mathbf{Q}^{-1}$  where  $\mathbf{Q}$  is the matrix of eigenvectors and  $\mathbf{\Sigma}$  is the diagonal matrix of eigenvalues. Notice that for any matrix  $\mathbf{A}$ , with SVD given by  $\mathbf{U}\mathbf{\Sigma}\mathbf{V}^T$ , we have the eigendecompositions  $\mathbf{A}^T\mathbf{A} = \mathbf{V}\mathbf{\Sigma}^2\mathbf{V}^T$  and  $\mathbf{A}\mathbf{A}^T = \mathbf{U}\mathbf{\Sigma}^2\mathbf{U}^T$ . These formulations are useful when  $\mathbf{A}$  is a tall skinny or a short wide matrix. In the case where  $\mathbf{\Sigma}$  contains no zero singular values, the SVD of  $\mathbf{A}$  can be more efficiently computed via the eigendecomposition of a smaller  $\mathbf{A}^T\mathbf{A}$  or  $\mathbf{A}\mathbf{A}^T$  matrix. Notice, for instance that once  $\mathbf{U}$  is computed, one can compute  $\mathbf{V}$  using  $\mathbf{A}^T$  and the inverse of  $\mathbf{\Sigma}$ :

$$\mathbf{A}^T\mathbf{U} = \mathbf{V}\mathbf{\Sigma} \Rightarrow \mathbf{V} = \mathbf{A}^T\mathbf{U}\mathbf{\Sigma}^{-1}$$

Via a similar relation, one can compute  $\mathbf{U}$  given  $\mathbf{V}$  using  $\mathbf{U} = \mathbf{A}\mathbf{V}\mathbf{\Sigma}^{-1}$ .

## 2.2. Principal component analysis.

Originally formulated by Pearson (1901), principal component analysis (PCA)<sup>3</sup> still plays an important role in modern statistics due to its simple geometric interpretation. Specifically, it is widely used for feature extraction and visualization of big data-sets comprising many interrelated variables. A classical statistical text on PCA is Jolliffe (2002), while more modern views and extensions are presented by Hastie, Tibshirani, and Friedman (2009), Murphy (2012) and Izenman (2008). Further, we want to point out the excellent review by Abdi and Williams (2010) and the recent seminal paper on linear dimensionality reduction by Cunningham and Ghahramani (2015).

The essential idea of PCA is to find a new set of uncorrelated variables that retain most of the information (total variation) present in the data. Figure 3 illustrates this for a two-dimensional example. Subplot (a) shows some fairly correlated data. The arrows indicate the principal directions of the data. It can be seen that the first arrow points into the direction which explains most of the variance, while the second arrow is orthogonal to the first one. Together, they span a new coordinate system so that the first axis accounts for most of the variance and the second for the remaining variance in the data. Subplot (b) shows the original data in this new coordinate system, represented by a new set of uncorrelated variables the so called principal components. The values of these new variables are called principal component scores or coordinates. The histograms indicate that most information (variation) is now captured by just the first principal component (PC).

<sup>3</sup>Also commonly known as Hotelling transform, Karhunen Loève, or proper orthogonal decomposition (POD).

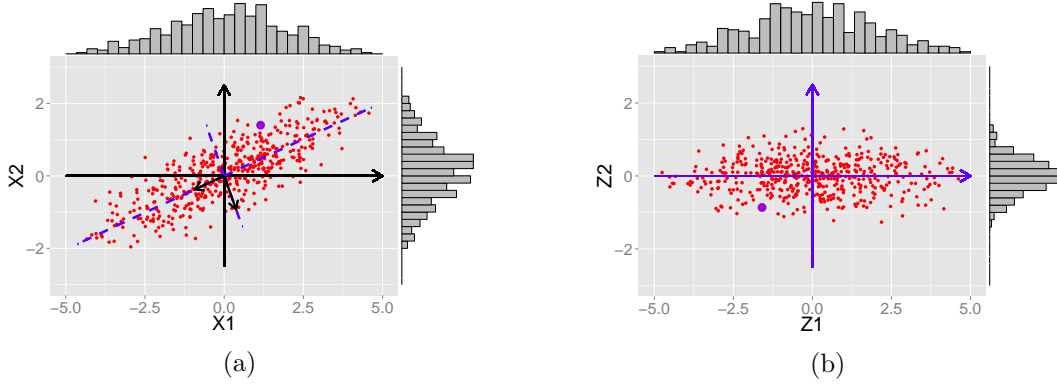


Figure 3: Illustration of PCA seeking to find a new set of uncorrelated variables. In (a) data and its two principal directions are shown. In (b) the new principal component variables are shown, indicating that the first component accounts for most of the variation in the data.

Given a data matrix  $\mathbf{X} \in \mathbb{R}^{n \times p}$  with  $n$  observations and  $p$  variables (column wise mean centered), the principal components can be expressed as a linear combination

$$\mathbf{z}_i = \mathbf{X}\mathbf{w}_i \quad (5)$$

where  $\mathbf{z}_i \in \mathbb{R}^n$  denotes the  $i$ 'th principle component and the  $i$ 'th principal direction is represented by the vector  $\mathbf{w}_i \in \mathbb{R}^p$ , where the elements of  $\mathbf{w}_i = (w_1, \dots, w_p)^T$  are the corresponding principal component coefficients or weights.

In summary, we seek that the first principal component explains most of the total variation in the data and that the following PCs are orthogonal to the previous ones, while explaining the remaining variance in descending order. Mathematically, this problem can be formulated either as a least square minimization or as variance maximization problem (Cunningham and Ghahramani 2015). However, both boil down to an eigenvalue problem. We follow the latter, and the more modern approach, i.e., maximizing the variance of the first principal component subject to the normalization constraint  $\|\mathbf{w}\|_2^2 = 1$  as follows

$$\mathbf{w}_1 = \max_{\|\mathbf{w}_1\|_2^2=1} \text{VAR}(\mathbf{X}\mathbf{w}_1) \propto \max_{\|\mathbf{w}_1\|_2^2=1} \|\mathbf{X}\mathbf{w}_1\|_2^2 \quad (6)$$

where  $\|\cdot\|_2$  denotes the induced  $\ell_2$  norm. The last term can then be expanded as

$$\mathbf{w}_1 = \max_{\|\mathbf{w}_1\|_2^2=1} \mathbf{w}_1^T (\mathbf{X}^T \mathbf{X}) \mathbf{w}_1 \quad (7)$$

revealing the resemblance (up to a scaling factor) of the inner term  $\mathbf{X}^T \mathbf{X}$  (also denoted as Gram matrix) with that of the covariance matrix  $\mathbf{C} \in \mathbb{R}^{p \times p}$ . Specifically, the sample covariance matrix is defined as

$$\mathbf{C} = \frac{1}{n-1} \mathbf{X}^T \mathbf{X}. \quad (8)$$

Considering that we constrained  $\|\mathbf{w}\|_2^2 = \mathbf{w}^T \mathbf{w} = 1$  to be a unit vector, we can rewrite (7) as

$$\mathbf{w}_1 = \max \frac{\mathbf{w}_1^T (\mathbf{X}^T \mathbf{X}) \mathbf{w}_1}{\mathbf{w}_1^T \mathbf{w}_1}. \quad (9)$$

From (9) we can draw the connection to the Rayleigh quotient<sup>4</sup>

$$\rho = \frac{\mathbf{w}^T \mathbf{C} \mathbf{w}}{\mathbf{w}^T \mathbf{w}} \quad (10)$$

where  $\mathbf{C}$  is a symmetric positive definite matrix, e.g., a covariance or correlation matrix. Now maximizing the Rayleigh quotient  $\rho$  is equivalent to

$$\max_{\mathbf{w}_1} \mathbf{w}_1^T \mathbf{C} \mathbf{w}_1 \quad \text{subject to} \quad \mathbf{w}_1^T \mathbf{w}_1 = 1 \quad (11)$$

and this can be solved using the method of Lagrange multipliers

$$\mathcal{L}(\mathbf{w}_1, \lambda_1) = \max_{\mathbf{w}_1, \lambda} (\mathbf{w}_1^T \mathbf{C} \mathbf{w}_1 - \lambda_1 (\mathbf{w}_1^T \mathbf{w}_1 - 1)). \quad (12)$$

Solving  $\mathcal{L}$  with respect to  $\mathbf{w}_1$  and  $\lambda_1$  leads to the well known eigenvalue problem

$$\mathbf{C} \mathbf{w}_1 = \lambda_1 \mathbf{w}_1. \quad (13)$$

Hence, the first principle direction for the mean centered matrix  $\mathbf{X}$  is given by the dominant eigenvector  $\mathbf{w}_1$ . More generally, the principle directions of the covariance matrix  $\mathbf{C}$  are the columns of the eigenvector matrix  $\mathbf{W} \in \mathbb{R}^{p \times p}$  and the corresponding eigenvalues  $\lambda$  are the diagonal elements of  $\mathbf{\Lambda} \in \mathbb{R}^{p \times p}$ . Interestingly, the eigenvalues express exactly the amount of variation explained by the principal components.

$$\mathbf{C} \mathbf{W} = \mathbf{\Lambda} \mathbf{W}. \quad (14)$$

More compactly, we can compute the principal components  $\mathbf{Z} \in \mathbb{R}^{n \times p}$  as

$$\mathbf{Z} = \mathbf{X} \mathbf{W}. \quad (15)$$

Hence, the matrix  $\mathbf{W}$  can also be interpreted as a projection matrix that maps the original observations to the new coordinates in the eigenspace. Since the eigenvectors have unit norm the projection should be purely rotational without any scaling; thus, the matrix  $\mathbf{W}$  is also denoted as a rotation matrix. However, we want to stress that the term ‘loading’ in general refers to the scaled eigenvectors

$$\mathbf{L} = \mathbf{W} \mathbf{\Sigma}^{0.5} \quad (16)$$

which, in some situations, provide a more insightful interpretation of the principal components.<sup>5</sup> The loading matrix  $\mathbf{L} \in \mathbb{R}^{n \times p}$  has the properties: a) the squared column sums equal the eigenvalues, and b) the squared row sums equal the amount of a variable’s variance explained.

In practice, we are often interested in a useful low-dimensional representation to reveal the coherent structure of the data. However, the decision of how many principal components to keep is subtle and often domain specific. Many different heuristics (e.g. scree plot) have been proposed [Jolliffe \(2002\)](#) and a recent mathematically refined approach is the method of the optimal hard threshold for singular values introduced by [Gavish and Donoho \(2014\)](#).

Note that the analysis of variables, which are measured in different units, can be misleading and cause undesirable interpretations. This is because the eigenvectors are not scale invariant. Thus, it is favorable to use the correlation matrix instead of the covariance matrix in general.

<sup>4</sup>The Rayleigh quotient is powerful concept from linear algebra and plays an import role in statistical learning, see for example [Yu, Tranchevent, and Moreau \(2011\)](#).

<sup>5</sup>Technically, the eigenvectors can be seen as direction cosines, while the corresponding eigenvalues describe the magnitude. By construction, the loading matrix aggregates both.



**The singular value decomposition to compute PCA.** In practice the explicit computation of the covariance or correlation matrix for massive data-sets can be expensive. A more computationally efficient approach to compute the principal components is the singular value decomposition, which avoids the (often) costly computation of the Gram matrix  $\mathbf{X}^T\mathbf{X}$ . As described in section 2.1, the eigenvalue decomposition of the inner and outer dot product of  $\mathbf{X} = \mathbf{U}\mathbf{S}\mathbf{V}^T$  can be related to the singular value decomposition as follows

$$\mathbf{X}^T\mathbf{X} = (\mathbf{V}\mathbf{S}\mathbf{U}^T)(\mathbf{U}\mathbf{S}\mathbf{V}^T) = \mathbf{V}\mathbf{\Sigma}\mathbf{V}^T \quad (17a)$$

$$\mathbf{X}\mathbf{X}^T = (\mathbf{U}\mathbf{S}\mathbf{V}^T)(\mathbf{V}\mathbf{S}\mathbf{U}^T) = \mathbf{U}\mathbf{\Sigma}\mathbf{U}^T \quad (17b)$$

where the eigenvalues  $\mathbf{\Sigma} = \mathbf{S}^2$  are the squared singular values. The eigenvectors of  $\mathbf{X}\mathbf{X}^T$  are given by the left singular vectors  $\mathbf{U}$  and the eigenvectors of  $\mathbf{X}^T\mathbf{X}$  are given by the right singular vectors  $\mathbf{V}$  of the matrix  $\mathbf{X}$ . Thus, from the SVD of  $\mathbf{X}$  we recover the rotation matrix  $\mathbf{W}$  and eigenvalues  $\mathbf{\Lambda}$  of the covariance matrix  $\mathbf{C}$  as  $\mathbf{\Lambda} = \frac{1}{n-1}\mathbf{S}^2$  and  $\mathbf{W} = \mathbf{V}$ . Moreover, the principal component scores can be computed as

$$\mathbf{Z} = \mathbf{X}\mathbf{W} = \mathbf{U}\mathbf{S}\mathbf{V}^T\mathbf{W} = \mathbf{U}\mathbf{S}. \quad (18)$$

### 2.3. Robust principal component analysis.

In the previous two section we have presented two closely related methods for dimensionality reduction, namely the singular value decomposition and principal component analysis. In fact, we have shown that PCA can be efficiently computed using the SVD. Moreover, we show in Section 4 that these methods can be used for noise reduction/removal, if the data are corrupted by i.i.d. Gaussian noise and the signal-to-noise ratio is sufficiently large. However, in many practical applications we face data with arbitrarily corrupted observations, e.g., shadows in images or moving objects in videos. In this case the resulting low-rank approximations can be poor, even if only a very few observations are corrupted. Figure 4 presents a toy example of such a possible situation.<sup>6</sup> Subplot (a) shows a grossly corrupted data matrix as the superposition of a half torus (b) and spike noise (c). Specifically, the corrupted ( $200 \times 200$ ) data matrix here is superimposed of a low-rank component ( $r = 3$ ) and some sparse component. The question arises, whether a corrupted data matrix  $\mathbf{A} \in \mathbb{R}^{m \times n}$  can be robustly separated into a low-rank matrix  $\mathbf{L} \in \mathbb{R}^{n \times m}$  and sparse matrix  $\mathbf{S} \in \mathbb{R}^{n \times m}$

$$\mathbf{A} = \mathbf{L} + \mathbf{S} \quad (19)$$

so that  $\mathbf{S}$  captures the perturbations. Indeed, Candès, Li, Ma, and Wright (2011) proved that it is possible to exactly separate such a data matrix into both its low-rank and sparse components, under rather broad conditions. Specifically, it is achieved by solving a convenient convex optimization problem, called principal component pursuit (PCP), minimizing a weighted combination of the nuclear norm  $\|\cdot\|_* := \sum_i \sigma_i$  (sum of the singular values) and the  $\ell_1$  norm  $\|\cdot\|_1 := \sum_{ij} |m_{ij}|$  as follows

$$\min_{\mathbf{L}, \mathbf{S}} \|\mathbf{L}\|_* + \lambda \|\mathbf{S}\|_1 \quad \text{subject to } \mathbf{A} - \mathbf{L} - \mathbf{S} = 0. \quad (20)$$

The arbitrary balance parameter,  $\lambda > 0$ , is typically chosen to be  $\lambda = 1/\sqrt{\max(n, m)}$ . Hence, the key to achieving such a matrix decomposition is  $\ell_1$  optimization. The PCP concept (20) is

<sup>6</sup>The **plot3D** package was utilized to produce 3D plots (Soetaert 2016).



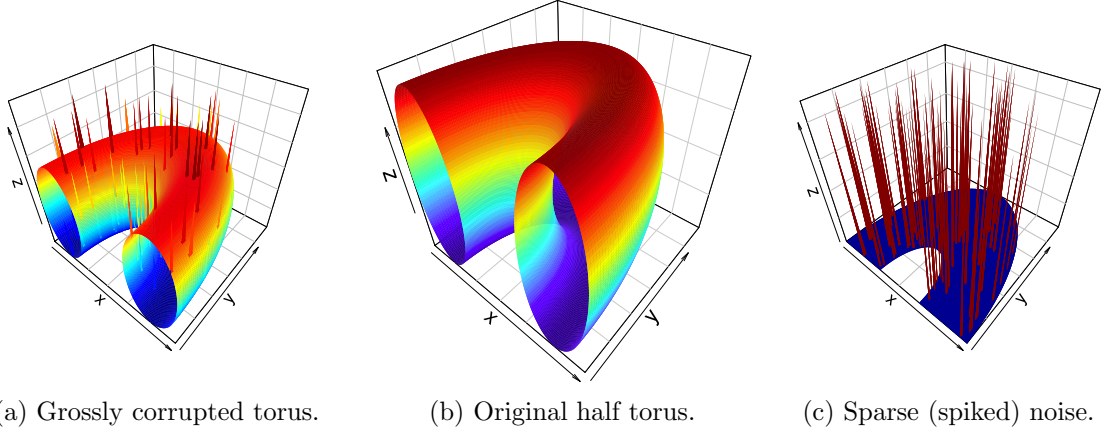
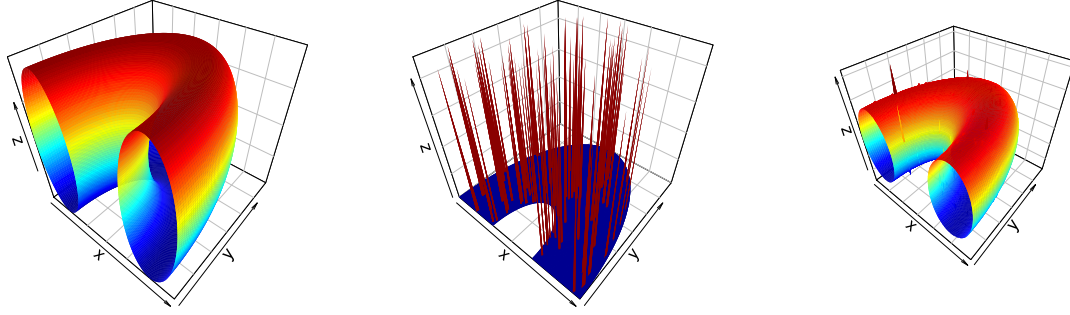


Figure 4: Toy example of a grossly corrupted data matrix. Subplot (a) shows the perturbed torus as a superposition of the half torus (b) and spike noise (c).

mathematically sound and has been applied successfully to images and videos (Wright, Ganesh, Rao, Peng, and Ma 2009). More generally the concept of robustly separating corrupted matrices is denoted as robust principal component analysis (RPCA). However, its biggest challenge is computational speed and efficiency, especially given the iterative nature of the optimization required. Bouwmans, Sobral, Javed, Jung, and Zahzah (2015) have identified more than 30 related algorithms to the original PCP approach. Most of these aim to overcome the computational complexity of the original algorithm, but there are meanwhile also algorithms extending and generalizing the above described separation problem. For instance, the inexact augmented Lagrange multiplier method (Lin, Chen, and Ma 2010) is a popular choice, with favorable computational and performance properties. This method essentially formulates the following Lagrangian function for the problem as stated in (20)

$$\mathcal{L}(\mathbf{L}, \mathbf{S}, \mathbf{Y}, \mu) = \|\mathbf{L}\|_* + \lambda \|\mathbf{S}\|_1 + \langle \mathbf{Y}, \mathbf{A} - \mathbf{L} - \mathbf{S} \rangle + \frac{\mu}{2} \|\mathbf{A} - \mathbf{L} - \mathbf{S}\|_F^2 \quad (21)$$

where  $\mu$  is a positive scalar and the matrix  $\mathbf{Y}$  is the Lagrange multiplier. Applying this method to the corrupted half torus presented in Figure 4, yields an exact separation into the low-rank and sparse components shown in Figure 5. The reconstruction error is 0.0003%, which is nearly negligible. In comparison, subplot (c) shows the low-rank approximation computed from a standard SVD, containing substantial defects.



(a) Low-rank component  $\mathbf{L}$ . (b) Sparse component  $\mathbf{S}$ . (c) SVD low-rank approximation.

Figure 5: Subplot (a) and (b) show the separation of the grossly corrupted Torus in Figure 4 using randomized robust PCA. The decomposition is nearly perfect and captures the original Torus faithfully. The normalized root mean squared error is as low as 0.0003%, while the SVD yields a poor reconstruction error of about 1.81%, shown in subplot (c).

The remarkable ability of separating a high-dimensional matrix into a low-rank and sparse matrix, makes robust principal component analysis a valuable tool. Typical applications can be found in image or video processing, as well as in bioinformatics. However, the method is computationally demanding due to the requirement of the reiterated computation of the SVD. Facilitating the randomized SVD algorithm instead can ease the computation substantially.

### 3. Randomized algorithms

The computational cost of computing the truncated SVD  $\mathbf{A}_k$  using a deterministic algorithm can be tremendous for massive data-sets. That is because the cost of a full SVD of an  $m \times n$  matrix is of the order  $O(mn^2)$ , from which the first  $k$  components can then be extracted to form  $\mathbf{A}_k$ . In contrast, randomized matrix techniques can be used to obtain an approximate rank- $k$  singular value decomposition at a cost of  $O(mnk)$ , substantially smaller than for a full SVD when the dimensions of  $\mathbf{A}$  are large. The randomized low-rank SVD approach can also be applied to accelerate the PCA computation. In this section we provide details on how this is accomplished.

#### 3.1. Randomized singular value decomposition.

We present details of the randomized low-rank SVD algorithm which comes with favorable error bounds relative to the optimal truncated SVD, as presented in the seminal paper by [Halko et al. \(2011b\)](#) and further analyzed and implemented in [Voronin and Martinsson \(2015\)](#). The algorithm can be conceptually divided into two stages. Given a real matrix  $\mathbf{A} \in \mathbb{R}^{m \times n}$  and a desired target rank  $k \ll m, n$ , the first stage makes use of randomization to build a low-dimensional subspace that approximately captures the column space of  $\mathbf{A}$ . This is achieved by simply drawing  $k$  random vectors  $\omega_1, \dots, \omega_k$  from a sub-Gaussian distribution, followed by computing a random projection of the data matrix

$$\mathbf{y}_i = \mathbf{A}\omega_i \quad \text{for } i=1,2,\dots,k. \quad (22)$$

The set of random projections  $\{\mathbf{y}_i\}$  serve as the approximate basis for the column space of the data matrix. This is because probability theory guarantees that random vectors, and hence the corresponding random projections, are linearly independent with high probability and quickly sample the range of a numerical rank deficient matrix  $\mathbf{A}$ . More compactly, the operation in (22) can be performed via one matrix–matrix multiplication:

$$\mathbf{Y} = \mathbf{A}\mathbf{\Omega} \quad (23)$$

where  $\mathbf{Y} \in \mathbb{R}^{m \times k}$  is the sample matrix and  $\mathbf{\Omega} \in \mathbb{R}^{n \times k}$  is a random sub-Gaussian matrix.

A natural basis can then be obtained by computing the economic QR decomposition of  $\mathbf{Y} = \mathbf{Q}\mathbf{R}$ , where  $\mathbf{Q} \in \mathbb{R}^{m \times k}$  is orthonormal and has the same column space as  $\mathbf{Y}$ . If  $k$  is large enough and close to the numeric rank  $\bar{r}$  of  $\mathbf{A}$ , then the resulting approximate basis  $\mathbf{Q}$  satisfies

$$\mathbf{A} \approx \mathbf{Q}\mathbf{Q}^T \mathbf{A}. \quad (24)$$

Notice that the statement in (24) is replaced by an equality when the number of samples drawn is large enough so that  $R(\mathbf{A}) \subseteq R(\mathbf{Y})$ . The second stage of the algorithm is concerned with obtaining the low-rank singular value decomposition from a small compressed matrix, which faithfully captures the relevant spectral information of the original data matrix. Therefore, we first project the input matrix  $\mathbf{A}$  onto the low-dimensional subspace

$$\mathbf{B} = \mathbf{Q}^T \mathbf{A} \quad (25)$$

to obtain the relatively small (if  $k \ll m, n$ ) matrix  $\mathbf{B} \in \mathbb{R}^{k \times n}$ . Computing any deterministic matrix factorization of this small compressed matrix is relatively inexpensive (if  $n$  is very large, it is possible to work with  $\mathbf{B}\mathbf{B}^T$  instead of directly with  $\mathbf{B}$ ). Hence one obtains the following approximate SVD by using a standard deterministic algorithm

$$\mathbf{B} = \tilde{\mathbf{U}}\mathbf{\Sigma}\mathbf{V}^T. \quad (26)$$

It then remains to recover the left singular vectors as follows

$$\mathbf{U} \approx \mathbf{Q}\tilde{\mathbf{U}}. \quad (27)$$

The justification for the randomized algorithm can be sketched as follows starting with (24):

$$\begin{aligned} \mathbf{A} &\approx \mathbf{Q}\mathbf{Q}^T \mathbf{A} \\ &\approx \mathbf{Q}\mathbf{B} \\ &\approx \mathbf{Q}\tilde{\mathbf{U}}\mathbf{\Sigma}\mathbf{V}^T \\ &\approx \mathbf{U}\mathbf{\Sigma}\mathbf{V}^T. \end{aligned} \quad (28)$$

Figure 6 illustrates the computational steps involved to compute the randomized singular value decomposition.

### 3.2. Computational considerations.

The approximation error of the randomized SVD can be controlled by two tuning parameters. First, it is beneficial to introduce a small oversampling parameter  $p$ , i.e., instead of using  $k$  random vectors,  $k + p$  random vectors are used to obtain the sample matrix  $\mathbf{Y}$ . Often, a

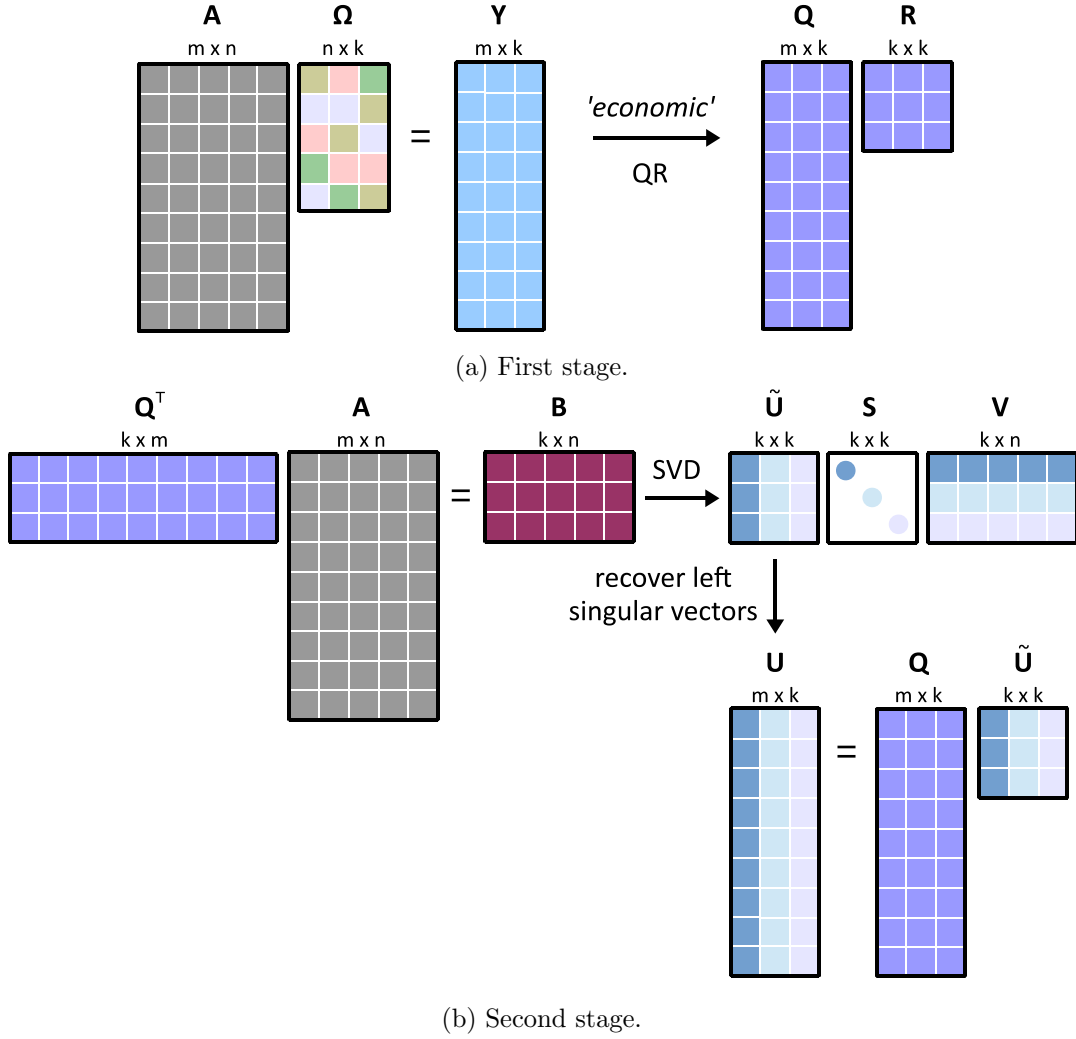


Figure 6: Schematic of the computational steps involved obtaining the randomized singular value decomposition.

fairly small oversampling parameter is sufficient, e.g.,  $p = 5, 10$ . In [Halko \*et al.\* \(2011b\)](#), the following practical error bound is derived:

$$\|\mathbf{A} - \mathbf{Q}\mathbf{Q}^T\mathbf{A}\| \leq \left[1 + 11\sqrt{k+p}\sqrt{\min(m,n)}\right] \sigma_{k+1} \quad (29)$$

where we compare the right hand side to  $\sigma_{k+1}$  in (4). The above bound holds with probability  $1 - 6p^{-p}$ , which justifies the use of a small oversampling parameter  $p$  relative to  $k$ .

The second method to improve the approximation involves the use of power sampling iterations. Instead of obtaining the sampling matrix  $\mathbf{Y}$  directly from the data matrix, one samples from a pre-processed matrix as follows

$$\mathbf{Y} = ((\mathbf{A}\mathbf{A}^T)^q \mathbf{A})\mathbf{\Omega} \quad (30)$$

where  $q$  is an integer determining the number of power iterations. A simple computation shows that  $(\mathbf{A}\mathbf{A}^T)^q \mathbf{A} = \mathbf{U}\mathbf{S}^{2q+1}\mathbf{V}$ . Hence, for  $q > 0$ , the modified sampling matrix has a

relatively fast decay of singular values even when the decay in  $\mathbf{A}$  is modest. The drawback is that additional matrix-matrix multiplications are required. However, when the singular values of the data matrix decay slowly, about  $q = 1, 2$  power iterations can considerably improve the approximation. For numerical reasons, in a practical implementation subspace iterations are used instead of power iterations (Gu 2015). The algorithm in Figure 7 summarizes an implementation with an oversampling parameter and subspace iterations.

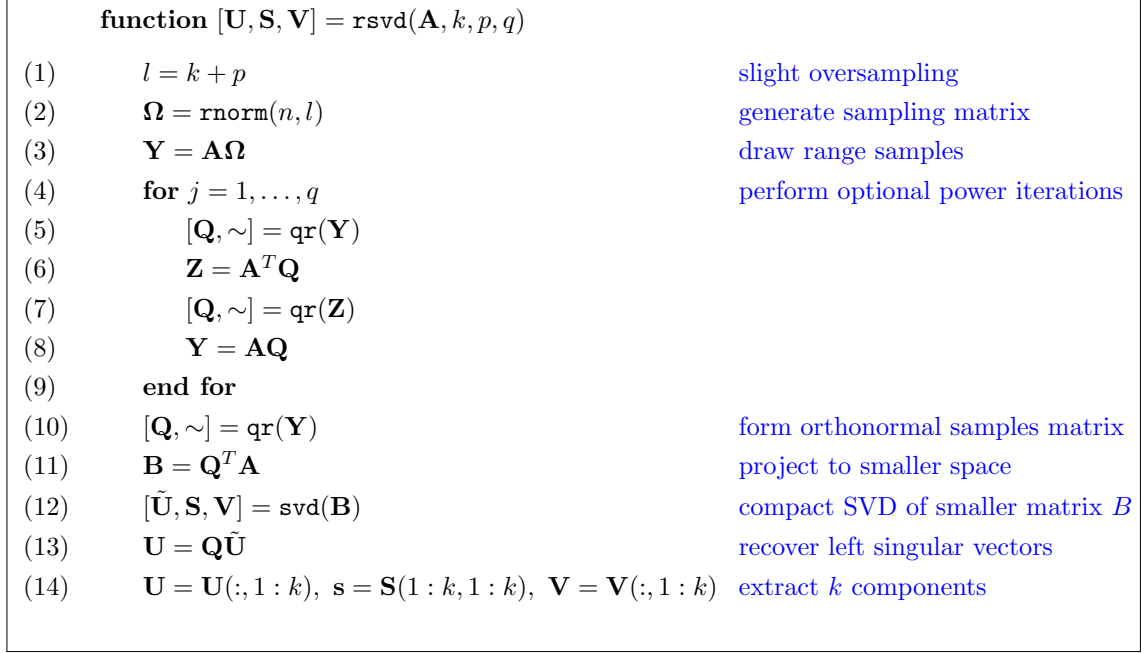


Figure 7: A randomized SVD algorithm.

*Remark 1.* The Gaussian or uniform distribution are common choices to generate  $\mathbf{\Omega}$ .

*Remark 2.* Numerical examples in Section 4 show that good default values for both the oversampling parameter and the number of subspace iterations are  $p = 10$  and  $q = 1$ .

*Remark 3.* The computational time can be further reduced by first computing the QR decomposition of  $\mathbf{B}^T$  and then computing the SVD of the even smaller matrix  $\mathbf{R} \in \mathbb{R}^{l \times l}$  or via the eigendecomposition of the  $l \times l$  matrix  $\mathbf{B}\mathbf{B}^T$  (see Voronin and Martinsson (2015) and Section 3.4 for further details).

**Error bounds.** The randomized algorithm for the low-rank SVD only approximates  $\mathbf{A}_k$ , the actual rank- $k$  truncated SVD, obtained from the full SVD of  $\mathbf{A}$ . The error bounds are worse than the optimal ones given in (4), but the practical results tend to be very close to optimal. In the algorithm in Figure 7, we compute the full SVD of  $\mathbf{B}$ , so it follows that  $\|\mathbf{A} - \mathbf{U}_k \mathbf{S}_k \mathbf{V}_k^T\| = \|\mathbf{A} - \mathbf{Q}\mathbf{Q}^T \mathbf{A}\|$ . In Halko *et al.* (2011b), the following error bound is derived:

$$\mathbb{E} [\|\mathbf{A} - \mathbf{U}_k \mathbf{S}_k \mathbf{V}_k^T\|] \leq \left[ \left( 1 + \sqrt{\frac{k}{p-1}} \right) \sigma_{k+1}^{2q+1} + \frac{e\sqrt{k+p}}{p} \left( \sum_{j>k} \sigma_j^{2(2q+1)} \right)^{\frac{1}{2}} \right]^{\frac{1}{2q+1}}$$

When the singular values  $\sigma_j$  for  $j > k$  are small in magnitude, the sum in the above formula is small and the bound approaches the theoretically optimal value of  $\sigma_{k+1}$  with increasing  $q$ .

Note again that the error in the approximate low rank SVD factorization obtained with the randomized algorithm coincides with the bound  $\|\mathbf{A} - \mathbf{Q}\mathbf{Q}^T\mathbf{A}\|$ . To control the error, one may proceed to buildup  $\mathbf{Q}$  by adding samples to expand  $\mathbf{Y}$  a step at a time, until the bound becomes small. A more intricate iterative procedure for building up  $\mathbf{Q}$  such that the bound holds to a specified tolerance, is presented in [Martinsson and Voronin \(2015\)](#).

### 3.3. Measurement matrices.

An essential computational step of the randomized algorithm is to construct a measurement matrix  $\mathbf{\Omega}$  that is used to sample the range of the input matrix. Therefore we rely on the properties of random vectors, which imply that the randomly generated columns of the measurement matrix are linearly independent with high probability. Indeed, this includes the whole class of sub-Gaussian random variables ([Rivasplata 2012](#)), including matrices with Bernoulli or uniform random entries. Specifically, sub-Gaussian random variables meet the Johnson-Lindenstrauss properties ([Johnson and Lindenstrauss 1984](#)), guaranteeing that the spectral information is preserved.

Due to its beautiful theoretical properties, the random Gaussian measurement matrix is the most prominent choice, consisting of independent identically distributed (iid)  $\mathcal{N}(0, 1)$  standard normal entries. In practice, however, uniform random measurements are sufficient and are less expensive to generate. The drawback is that dense matrix multiplications are expensive for large matrices, with computational cost of  $O(mnk)$ . However, BLAS operations tend to be highly scalable and computations could be substantially accelerated with parallel or distributed processing, e.g., a graphics processing unit (GPU) implementation ([Erichson and Donovan 2016](#); [Voronin and Martinsson 2015](#)).

[Woolfe et al. \(2008\)](#) proposed another computationally efficient approach, exploiting the properties of a structured random measurement matrix. For instance, using a subsampled random Fourier transform measurement matrix reduces the computational costs from  $O(mnk)$  to  $O(mn \log(k))$ .

In some situations, an even simpler construction of the sample matrix  $\mathbf{Y}$  is sufficient. For instance,  $\mathbf{Y}$  can be constructed by choosing  $k$  random columns without replacement from  $\mathbf{A}$ , which makes the expensive matrix multiplication redundant. This approach is particularly efficient if the information is uniformly distributed over the data matrix ([Cohen, Lee, Musco, Musco, Peng, and Sidford 2015](#)), e.g., in images or videos. However, if the data matrix is highly sparse, this approach is prone to fail.

### 3.4. Randomized principal component analysis.

The information in the data is often explained by just the first few dominant principal components, and thus the randomized singular value provides an efficient and fast algorithm for computing the first  $k$  principal components. This approach is denoted as randomized principal component analysis (rPCA), introduced by [Rokhlin, Szlam, and Tygert \(2009\)](#) and [Halko, Martinsson, Shkolnisky, and Tygert \(2011a\)](#). See also [Szlam, Kluger, and Tygert \(2014\)](#) for some interesting implementation details. Instead of using the randomized SVD Algorithm in Figure 7 directly where the SVD of  $\mathbf{B}$  is computed, we facilitate a modified Algorithm

proposed by Voronin and Martinsson (2015), which utilizes instead the eigendecomposition of the smaller  $\mathbf{B}\mathbf{B}^T$  matrix.

Specifically, for use in PCA, we compute the approximate randomized low-rank eigenvalue decomposition of  $\mathbf{X}^T\mathbf{X}$  given the rectangular mean centered matrix  $\mathbf{X}$ . Note that if  $\mathbf{X} = \mathbf{U}\mathbf{\Sigma}\mathbf{V}^T$ , then  $\mathbf{X}^T\mathbf{X} = \mathbf{V}\mathbf{\Sigma}^2\mathbf{V}^T \approx \mathbf{V}_k\mathbf{\Sigma}_k^2\mathbf{V}_k^T$  and  $\mathbf{X}\mathbf{A}^T = \mathbf{U}\mathbf{\Sigma}^2\mathbf{U}^T \approx \mathbf{U}_k\mathbf{\Sigma}_k^2\mathbf{U}_k^T$ . Performing such an eigendecomposition for an  $m \times n$  matrix with many columns would be expensive, since  $\mathbf{X}^T\mathbf{X}$  is  $n \times n$ . On the other hand, the first  $k$  singular vectors and values of  $\mathbf{A}$  are approximately captured by  $\mathbf{B} = \mathbf{Q}^T\mathbf{X}$  where  $\mathbf{Q}$  is such that  $\mathbf{Q}\mathbf{Q}^T\mathbf{X} \approx \mathbf{X}$ . The  $l \times n$  matrix  $\mathbf{B}$  could still be large, so instead we can work with the  $l \times l$  matrix  $\mathbf{B}\mathbf{B}^T$ . Notice that if  $\mathbf{B} = \tilde{\mathbf{U}}\tilde{\mathbf{\Sigma}}\tilde{\mathbf{V}}^T$ , which we do not compute, then  $\mathbf{B}\mathbf{B}^T = \tilde{\mathbf{U}}\tilde{\mathbf{\Sigma}}^2\tilde{\mathbf{U}}^T$ . Suppose that we instead construct the eigendecomposition of  $\mathbf{B}\mathbf{B}^T = \tilde{\mathbf{W}}\tilde{\mathbf{S}}\tilde{\mathbf{W}}^T$ . It follows that  $\tilde{\mathbf{\Sigma}} = \tilde{\mathbf{S}}^{\frac{1}{2}}$  and that  $\text{trunc}(\tilde{\mathbf{\Sigma}}, k) \approx \text{trunc}(\tilde{\mathbf{S}}, k)$ . The first  $k$  left singular vectors can be recovered via the computation  $\mathbf{U}_k = \text{trunc}(\mathbf{Q}\tilde{\mathbf{W}}, k)$ . Employing the expression from section 2.1, we find that the first  $k$  right eigenvectors are approximately recovered via  $\mathbf{V}_k = \text{trunc}(\mathbf{B}^T\tilde{\mathbf{W}}\tilde{\mathbf{S}}^{-1}, k) = \text{trunc}(\mathbf{B}^T\tilde{\mathbf{W}}\tilde{\mathbf{S}}^{-\frac{1}{2}}, k)$ . Note that in practice, if only the eigendecomposition of  $\mathbf{X}^T\mathbf{X}$  or  $\mathbf{X}\mathbf{X}^T$  is needed, then only one of  $\mathbf{V}_k$  or  $\mathbf{U}_k$  needs to be computed.

The procedure is summarized in Algorithm 8 and the key difference are in lines 12 – 15.

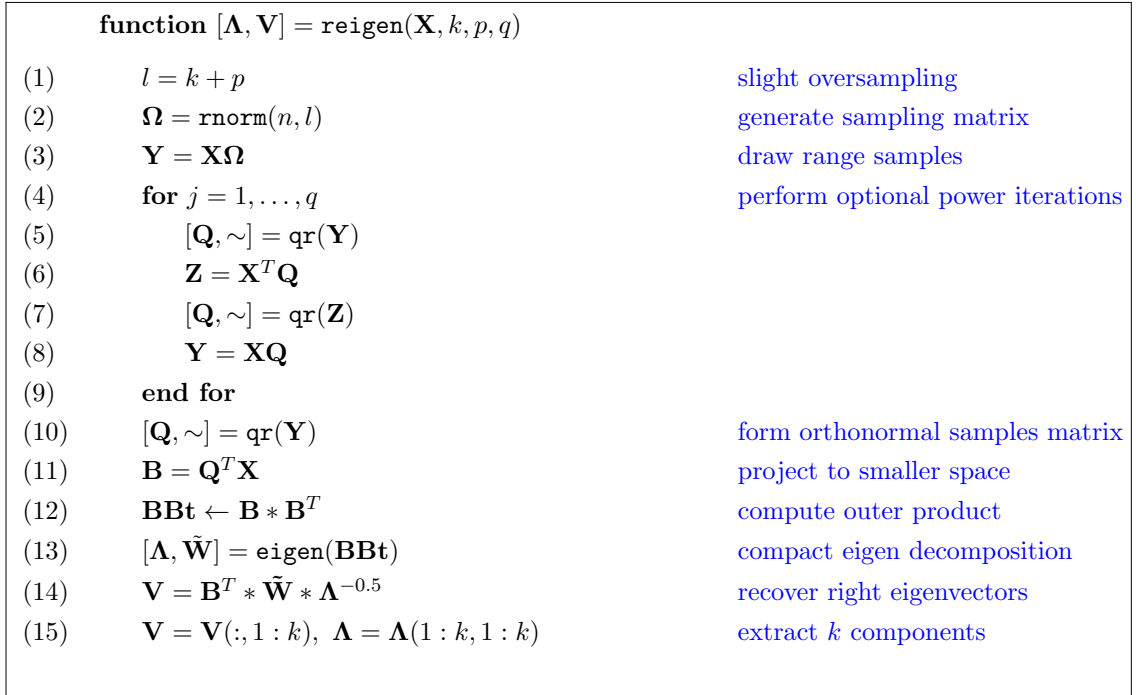


Figure 8: A randomized eigen algorithm.

## 4. Numerical Examples

In this section, we demonstrate how the randomized matrix algorithms work in practice. We illustrate the performance of our routines using several standard examples and compare the results to the corresponding deterministic R functions. Section 4.1 starts with a classic example



showing how the randomized singular value decomposition function `rsvd()` can be used for image compression. Sections 4.2 and 4.3 present two examples illustrating the randomized principal component analysis routine `rpca()`. The latter example involves a large dense matrix and highlights the computational advantage of randomized PCA. Section 4.4 introduces the randomized robust principal component analysis function `rrpca()`. Finally, section 4.5 investigates the performance of the `rsvd()` function, showing speed-ups ranging from 5 to 150 times.<sup>7</sup> In the following it is assumed that the `rsvd` package is installed and loaded.

```
R> install.packages("rsvd")
R> library("rsvd")
```

#### 4.1. SVD example: Image compression.

The singular value decomposition can be used to obtain a low-rank approximation to high-dimensional data. Image compression is a simple and illustrative example of this.<sup>8</sup> While images often feature a high-dimensional ambient space, the underlying structure can be represented by a very sparse model. This means that most natural images can be faithfully recovered from a relatively small set of basis functions. The `rsvd` library provides a  $1600 \times 1200$  grayscale image, which is used in to following to demonstrate this using both the standard and randomized SVD algorithms.

```
R> data(tiger)
R> image(tiger, col = gray((0:255)/255))
```

A grayscale image may be thought of as a real-valued matrix  $\mathbf{A} \in \mathbb{R}^{m \times n}$ , where  $m$  and  $n$  are the number of pixels in the vertical and horizontal directions, respectively. To compress the image we must first decompose the image. The singular vectors and values provide a hierarchical representation of the image in terms of a new coordinate system defined by dominant correlations within the image. Thus, the number of singular vectors used for approximation poses a trade-off between the compression rate (i.e., the number of singular vectors to be stored) and the image details. First, the R base `svd()` function is used to compute the singular value decomposition

```
R> k <- 100
R> tiger.svd <- svd(tiger, nu=k, nv=k)
```

The `svd()` function returns three objects: `u`, `v` and `d`. The first two objects are  $m \times k$  and  $n \times k$  arrays, namely the truncated right and left singular vectors. The latter object is a 1-D array comprising the singular values in descending order. Now, the dominant  $k = 100$  singular values are retained to approximate/reconstruct ( $\mathbf{A}_k = \mathbf{U}_k \mathbf{D}_k \mathbf{V}_k^T$ ) the original image

```
R> tiger.re <- tiger.svd$u %*% diag(tiger.svd$d[1:k]) %*% t(tiger.svd$v)
R> image(tiger.re, col = gray((0:255)/255))
```

The normalized root mean squared error (nrmse) is a common measure for the reconstruction quality of images (Fienup 1997), computed as

```
R> nrmse <- sqrt(sum((tiger - tiger.re)**2) / sum(tiger**2))
```

Using only the first  $k = 100$  singular values/vectors, the quality of the reconstructed image is

---

<sup>7</sup>The `microbenchmark` package is utilized for evaluating the computational time in the following (Mersmann, Beleites, Hurling, and Friedman 2015).

<sup>8</sup>Among the many strategies to compress or denoise images, the singular value decomposition is one prominent tool, although it is certainly not the most effective.

quite accurate with an nrmse as low as 0.121. This illustrates that in general natural images admit a very compact representation. However, using the base SVD algorithm for this example requires a relatively high computational time. Hence, this approach might not be practical for high-resolution images, e.g., 4K or 8K images. Utilizing the randomized algorithm instead can ease the computational time substantially. The provided `rsvd()` function can be used as a plug-in function for the base `svd()` function, in order to compute the near-optimal low-rank singular value decomposition

```
R> tiger.rsvd <- rsvd(tiger, k=k)
```

Similar to the base SVD function, the `rsvd()` function returns three objects: `u`, `v` and `d`. Again, `u` and `v` are  $m \times k$  and  $n \times k$  arrays containing the approximate right and left singular vectors and `d` is a 1-D array comprising the  $k$  singular values in descending order. The approximation accuracy of the rSVD algorithm can be controlled by two parameters  $p$  and  $q$ . The former is an oversampling parameter and the latter controls the number of subspace iterations. Specifically, if the singular value spectrum decays slowly, an increased number of subspace iterations can improve the accuracy. However, in practice we have not encountered a situation requiring  $q > 3$ . By default the parameters are set to  $p = 10$  and  $q = 1$ . Again, the approximated image and its reconstruction quality can be obtained as

```
R> tiger.re <- tiger.rsvd$u %*% diag(tiger.rsvd$d) %*% t(tiger.rsvd$v)
R> nrmse <- sqrt(sum((tiger - tiger.re)**2) / sum(tiger**2))
```

The reconstruction quality is similar, with an insignificantly larger nrmse of about 0.125; however, the randomized SVD algorithm is substantially faster. Figure 9 presents the results of the image approximation using both the deterministic and randomized SVD algorithm. By visual inspection no significant difference can be seen between the approximations using the deterministic and the randomized SVD algorithms (with  $q = 1$ ). However, it can be seen that the quality slightly suffers by excluding the computation of at least one subspace iteration.

Figure 10 shows both the corresponding singular values and the computational time. First it can be seen that the rSVD algorithm faithfully captures the true singular values with  $q = 1, 2$ . However, without computing subspace iterations, the singular values fall off slightly. Subplot (b) shows that an average speed-up of about 3.5 – 10 is achieved. The computational gain can be much larger for images of higher resolutions, i.e, bigger matrices.

The singular value decomposition is also a numerically reliable tool for extracting a desired signal from noisy data. The central idea is that the small singular values mainly represent the noise, while the dominant singular values represent a filtered (less noisy) signal. Thus, the low-rank SVD approximation can be used to denoise data matrices. To demonstrate this concept, the original image is first corrupted with additive white noise. Then, the underlying image (signal) is approximated using again the first  $k = 100$  singular vectors, illustrated in Figure 11. The nrmse indicates an improvement by about 15%.

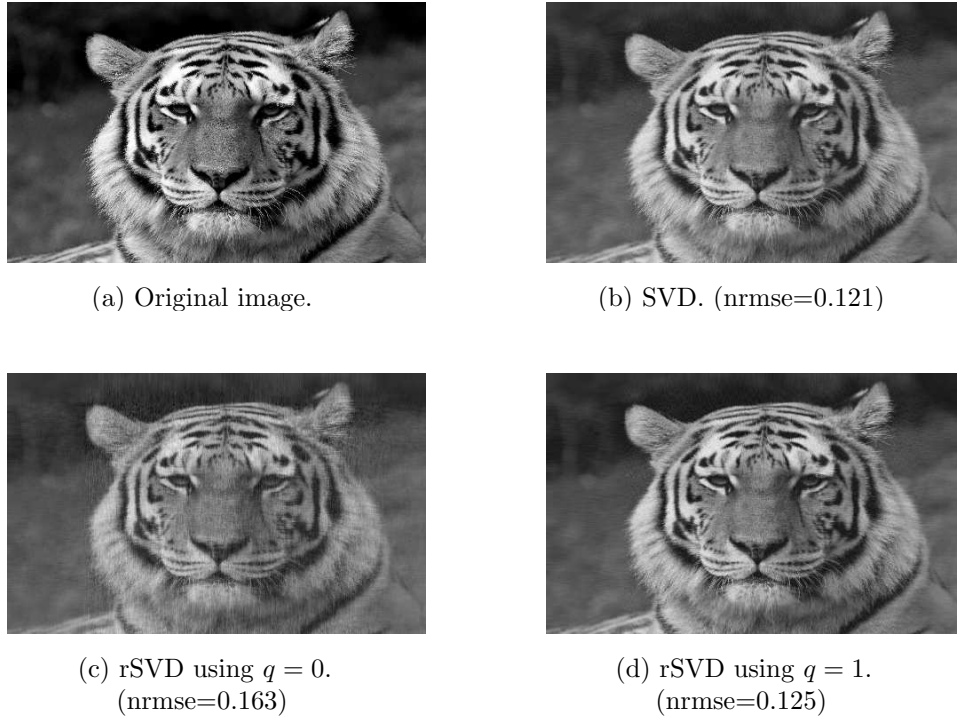


Figure 9: Image compression using the SVD. Subplot a) shows the original image and subplots (b), (c) and (d) show the reconstructed image using the dominant  $k = 100$  singular vectors by both the deterministic and randomized SVD algorithm. The reconstruction quality using  $q = 1$  subspace iterations is insignificant compared to the deterministic SVD algorithm.

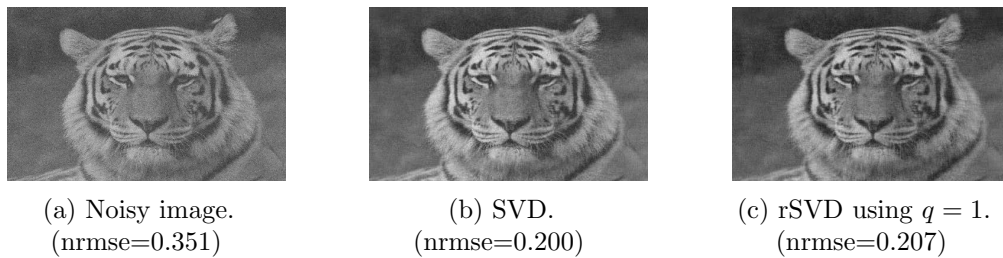


Figure 11: Image denoising using the singular value decomposition. Both the deterministic and randomized SVD reduce the error by about 15%.

The `rsvd()` function provides Gaussian and uniform (default) measurement matrices. The different options can be selected via the optional argument `sdist=c("normal", "uniform")`. While there is no significant practical difference in terms of accuracy, the generation of uniform samples is slightly more computationally efficient. See `?rsvd` for further details about the `rsvd()` function.

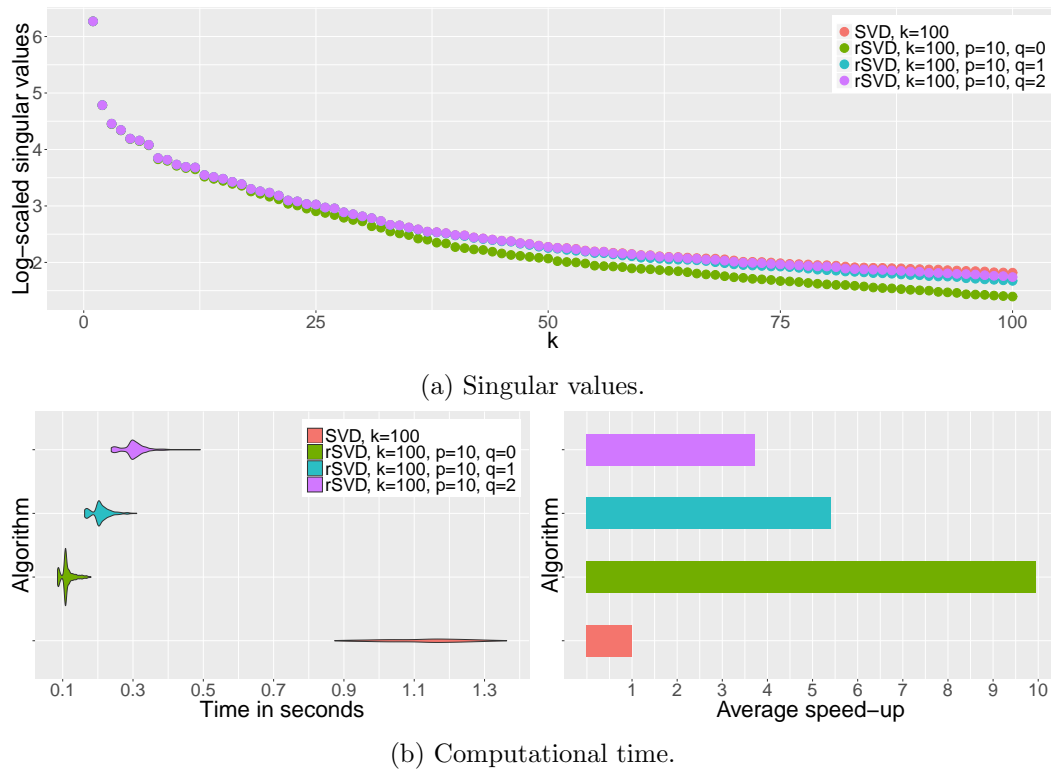


Figure 10: Subplot (a) shows the dominant log-scaled singular value spectrum of the image.

Subplot (b) shows the corresponding computational time for the deterministic and randomized SVD algorithm. The randomized routines achieve a substantial speed-up averaged over 200 runs.

#### 4.2. PCA example: Edgar Anderson’s Iris Data.

The function `rpca()` is designed as a substitute for the `stats::prcomp()` function, one of the standard methods to compute the principal component analysis in R. The key difference is that a randomized algorithm is used to perform the underlying computations. By default, the choice of whether to use the randomized or base SVD algorithm is made automatically. If the target-rank  $k > n/1.5$  the randomized algorithm is in general inefficient, and the deterministic SVD algorithm is favored.

In the following we use the famous `iris` data set, collected by [Anderson \(1935\)](#), to demonstrate the usage of the `rpca()` function. The data set comprises 50 observations from each of 3 species of iris: ‘setosa’, ‘versicolor’, and ‘virginica’. Each observation is a vector of values, measured in centimeters, of the variables ‘sepal length’, ‘sepal width’, ‘petal length’, and ‘petal width’, respectively.

```
R> data(iris)
R> head(iris, 2)
```

	Sepal.Length	Sepal.Width	Petal.Length	Petal.Width	Species
1	5.1	3.5	1.4	0.2	setosa
2	4.9	3.0	1.4	0.2	setosa

Following [Venables and Ripley \(2002\)](#), first the log transformed measurements are computed

```
R> log.iris <- log( iris[ , 1:4] )
```

which is a standard skewness transformation. Our primary aim here is to visualize the data in 2-D space using the first two ( $k = 2$ ) principal components.

```
R> iris.rpca <- rpca(log.iris, k=2)
```

By default, the data are mean centered and standardized, i.e., `center = TRUE` and `scale = TRUE`.<sup>9</sup> This means that the correlation matrix is implicitly computed here. Set `scale = FALSE` to use the implicit covariance matrix instead. The returned object of the `rpca()` function has the same summary, print and plot capabilities as `prcomp()`. For example the summary function shows

```
R> summary(iris.rpca)
```

	PC1	PC2
Explained variance	2.933	0.907
Standard deviations	1.712	0.952
Proportion of variance	0.733	0.227
Cumulative proportion	0.733	0.960
Eigenvalues	2.933	0.907

Thus, about 73% of the variability in the data is explained by just the first PC and about 23% by the second. Note, that the explained variance of the principal components corresponds exactly to the eigenvalues. In addition, the print function shows the variable loadings on the PCs. For instance, the first PC is best explained by ‘sepal length’, ‘petal length’ and ‘petal width’, while ‘sepal width’ loads onto the second component.

```
R> print(iris.rpca)
```

Standard deviations:

```
[1] 1.712 0.952
```

Eigenvalues:

```
[1] 2.933 0.907
```

Rotation:

	PC1	PC2
Sepal.Length	0.504	-0.455
Sepal.Width	-0.302	-0.889
Petal.Length	0.577	-0.034
Petal.Width	0.567	-0.035

Two widely used methods for visualizing the results of the principal component analysis are the correlation- and bi-plot. Relying on the **ggplot2** package ([Wickham 2009](#)), the correlation plot for the first and second principal component can be produced as follows

---

<sup>9</sup>Note, that the `prcomp()` function has by default the arguments `center = TRUE` and `scale = FALSE`.

```
R> ggcorplot(iris.rpca, pcs=c(1,2))
```

In order to create the biplot, the principal component scores (rotated variables) must be computed. This can be achieved by passing the argument `retx=TRUE` to the `rpca()` function. However, this requires re-computation and instead we use the provided `predict` function

```
R> iris.rpca$x <- predict(iris.rpca, log.iris)
```

Then the biplot is obtained as

```
R> ggbiplot(iris.rpca, groups = iris$Species)
```

Figure 12 shows the two plots. The correlation plot on the left visualizes the original variables by their correlation with the principal components (Abdi and Williams 2010). It can be seen that the variable ‘sepal width’ is most strongly correlated with the first two PCs. Moreover, it reveals the inter-relationships between the original variables. Clearly, the variables ‘petal length’ and ‘petal width’ are highly correlated, i.e., they carry redundant information. Whereas, ‘sepal width’ is only slightly correlated with the other variables. The correlations can be also computed as row sums of the squared eigenvectors, e.g., `rowSums(iris.rpca$rotation**2)`. The biplot represents both the observations and variables in eigenspace, i.e., it is a scatter plot of the principal component scores overlaid with the variable loadings. In particular, the biplot may help to reveal underlying patterns. For instance, here ‘setosa’ is distinct from the two other species. Further, the first PC is mainly explained by ‘sepal length’, ‘petal length’ and ‘petal width’, as noted before. An excellent general reference for biplots is Greenacre (2010). See also the help file `?rpca` for more details about the randomized PCA routine.

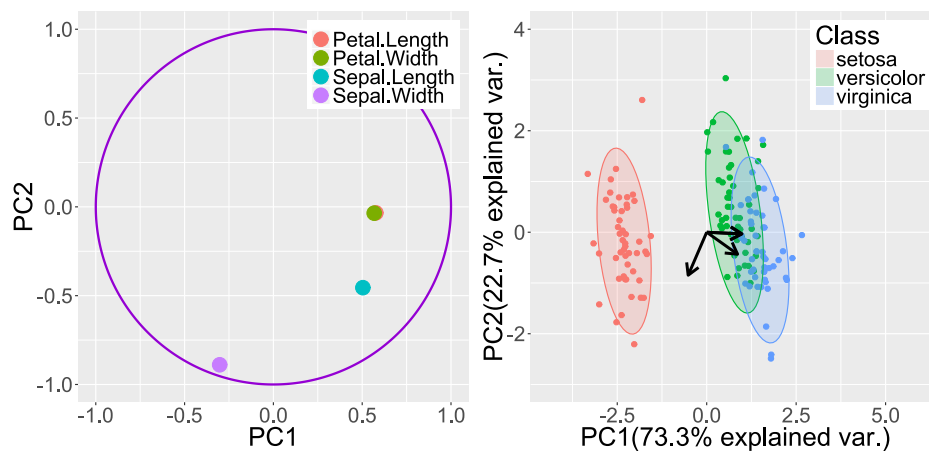


Figure 12: The left subplot visualizes the correlations of the original variable with the PCs. The biplot on the right plots the principal component scores, overlaid with a plot showing the principal directions.

### 4.3. PCA example: Eigenfaces.

One of the most striking demonstrations of PCA are eigenfaces, first studied by Kirby and Sirovich (1990). The aim is to extract the most dominant correlations between different faces from a large set of facial images. Specifically, the resulting columns of the rotation matrix (i.e., the eigenvectors) represent ‘shadows’ of the faces, called eigenfaces. This concept is illustrated

by using Kaggle's facial keypoints detection data-set<sup>10</sup>. The data-set comprises 7050 grayscale images of dimension  $96 \times 96$ , cropped and aligned. Each image is stored as a column vector of dimension 9216. The data-set can be loaded as

```
R> download.file("https://github.com/Benli11/data/raw/master/R/faces.RData",
"faces.RData")
```

```
R> load("faces.RData")
```

and then the 1st face can be displayed as

```
R> face <- matrix(rev(faces[,1]), nrow=96, ncol=96)
```

```
R> image(face, col=gray((0:255)/255))
```

Now, the randomized PCA algorithm can be facilitated to extract, for instance, the dominant  $k = 20$  eigenfaces as follows

```
R> faces.rpca <- rpca(t(faces), k=20, scale=FALSE)
```

Note, since the faces were stored as columns, we have to transpose the data matrix so that each column corresponds to a pixel location in space. Here, the analysis is performed on the covariance matrix by setting the argument `scale=FALSE`. The summary is as follows

```
R> summary(faces.rpca)
```

	PC1	PC2	PC3	...
Explained variance	8280837.158	3461939.368	2918616.418	...
Standard deviations	2877.644	1860.629	1708.396	...
Proportion of variance	0.295	0.123	0.104	...
Cumulative proportion	0.295	0.418	0.522	...
Eigenvalues	8280837.158	3461939.368	2918616.418	...

Just the first 3 PCs explain about 52% of the total variation in the data, while the first 20 PCs explain more than 75%. The summary can be visualized using either the provided `standard plot()` or the pretty plot functions shown in Figure 13.

```
R> ggscreeplot(faces.rpca)
```

```
R> ggscreeplot(faces.rpca, "cum")
```

```
R> ggscreeplot(faces.rpca, type="ratio")
```

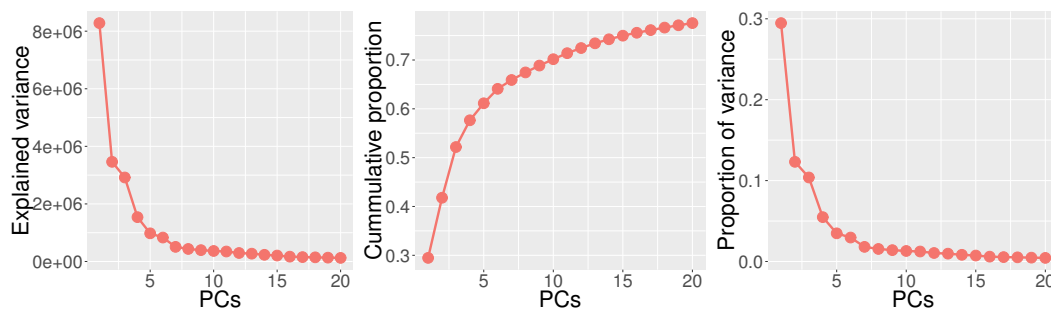


Figure 13: The left plot shows the eigenvalues (explained variance) in decaying order, the middle plot shows the cumulative proportion of the explained variance, while the right plot shows the proportion explained by the principal components.

<sup>10</sup><https://www.kaggle.com/c/facial-keypoints-detection>



Finally, the eigenvectors can be visualized as eigenfaces, e.g., the first eigenvector (eigenface) is displayed as follows

```
R> eigenface <- matrix(rev(faces.rpca$rotation[,1]), nrow=96, ncol=96)
R> image(eigenface, col=gray((0:255)/255))
```

The mean face is provided as the object `center`, and displayed as

```
R> meanface <- matrix(rev(faces.rpca$center), nrow=96, ncol=96)
R> image(meanface, col=gray((0:255)/255))
```

Figure 14 shows the first 4 dominant eigenfaces, computed with both the `prcomp()` and the `rpca()` function using different tuning parameters. Using rPCA without computing subspace iterations leads to degenerated eigenfaces. However, the true eigenfaces can be faithfully approximated by computing just one ( $q = 1$ ) subspace iteration. The corresponding computational timings and the standard deviations are shown in Figure 15. Here, we see the clear advantage of the randomized algorithm. It just takes about 4 to 6 seconds to compute the approximate dominant eigenfaces, while the deterministic `prcomp()` function requires about 160 seconds. This is a speed-up of about 33 times.

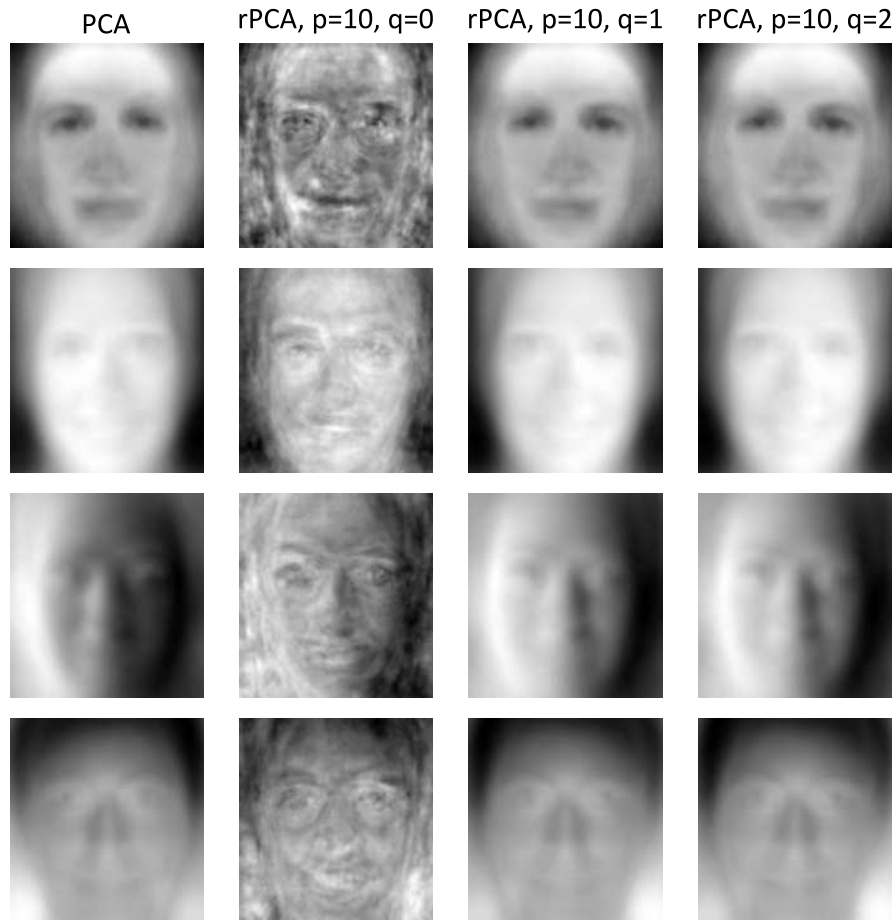


Figure 14: Dominant  $k = 4$  eigenfaces computed with both the `prcomp()` and `rpca()` functions using different tuning parameters.

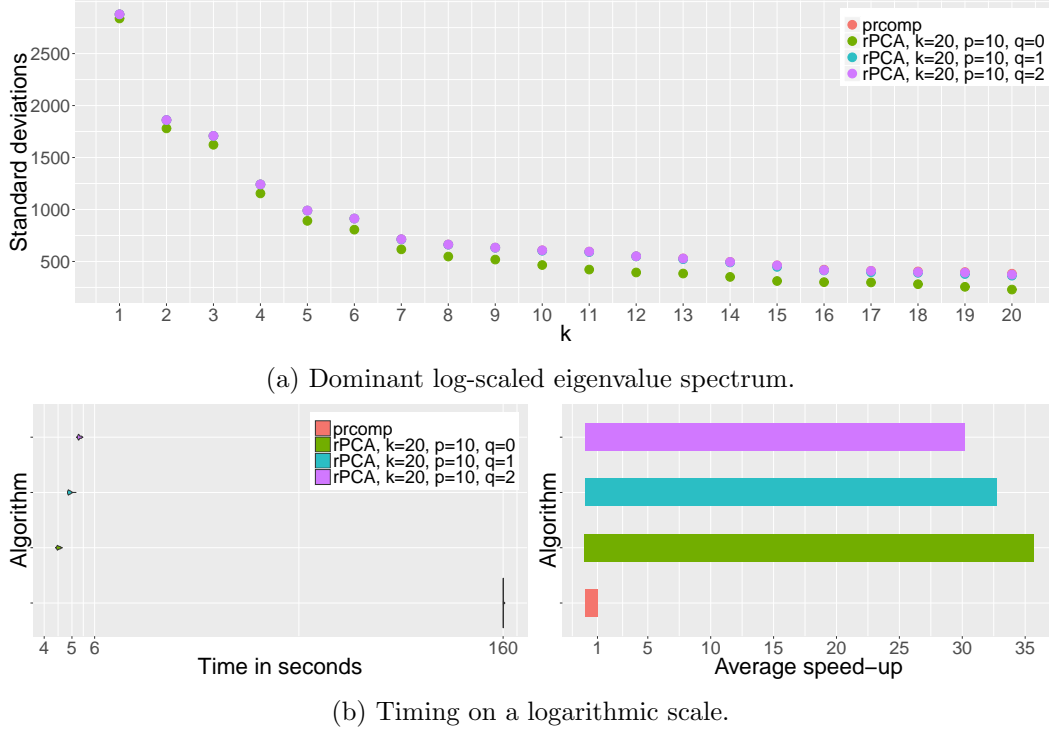


Figure 15: Subplot (a) shows the standard deviations and (b) shows the corresponding computational times for the deterministic and randomized PCA algorithm. The randomized algorithms achieves an about 33 fold speed-up compared to the deterministic PCA algorithm.

#### 4.4. Robust PCA example: Foreground/background separation.

In the following we demonstrate the randomized RPCA algorithm for video foreground/background separation, a problem studied widely in the computer vision community (Bouwman and Zahzah 2014). Background modeling is a fundamental task in computer vision used to detect moving objects in a given video stream from a static camera. The basic idea is that dynamic pixels in successive video frames are considered as foreground objects, whereas static pixels are considered part of the background. Thus the foreground can be found in a video by removing the background. However, background estimation is a challenging task due to the presence of foreground objects or variability in the background itself. One way to tackle this challenge is to exploit the low-rank structure of the background, while considering foreground objects as outliers. A solution to this problem is provided by the robust principal component analysis, which separates a matrix into a low-rank (background) and sparse component (representing the activity in the scene).<sup>11</sup> An example surveillance video (Goyette, Jodoin, Porikli, Konrad, and Ishwar 2012) containing 200 grayscale frames of size  $176 \times 144$  can be loaded as follows

```
R> download.file(https://github.com/Benli11/data/raw/master/R/highway.RData",
"highway.RData")
R> load("highway.RData")
```

<sup>11</sup>A general drawback of RPCA methods is that they rely on one or more tuning parameters, although, the default values are suitable in general.

Each frame is stored as a flattened column vector. For instance the 200th frame can be displayed as

```
R> image(matrix(highway[,200], ncol=144 , nrow=176), col = gray((0:255)/255))
```

Now, let's assume that the background is the low-rank component, as discussed above. This is fairly reasonable, since the camera is fixed and the background only gradually changes over time. The separation is then obtained as follows

```
R> highway.rrpca <- rrpca(highway, k=1, p=0, q=1, trace=TRUE)
```

The `rrpca()` function returns two objects: `L` and `S`, which are both  $m \times n$  arrays. The first object contains the low-rank component and the latter the sparse component. Thus, the results can be illustrated by displaying an example frame of both the low-rank and sparse matrix

```
R> image(matrix(highway.rrpca$L[,200] , ncol=144 , nrow=176),  
col = gray((0:255)/255))  
R> image(matrix(highway.rrpca$S[,200] , ncol=144 , nrow=176),  
col = gray((0:255)/255))
```

shown in Figure 16. It clearly can be seen that the algorithm treats the foreground objects as sparse components, representing outlying entries in the data matrix. Thus the algorithm faithfully separates the video into its two components. Figure 17 shows the convergence and



Figure 16: Foreground/background separation of a video using rRPCA. The left subplot is showing the true raw video frame separated into the low-rank component (background) and a sparse component capturing foreground objects.

computational time of the RPCA algorithm using both the deterministic and the randomized SVD algorithm. The randomized algorithm converges after about 18 iterations. The deterministic RPCA algorithm converges slightly faster, i.e., it requires fewer iterations. However, each iteration is substantially more expensive. Hence the randomized RPCA algorithm achieves an average-speed up of about a factor of 3. Also the convergence is smoother than that of the deterministic algorithm, a beneficial feature of randomized algorithms. The gain on larger video streams is even more significant.

It is interesting to note here that the oversampling parameter  $p$  can lead implicitly to regularization of the RPCA algorithm. Moreover, we want to stress that the randomized RPCA algorithm only achieves accurate results, if the singular value spectrum is rapidly decaying, i.e., the data exhibit a low-rank structure. See the help file `?rrpca` for more details.

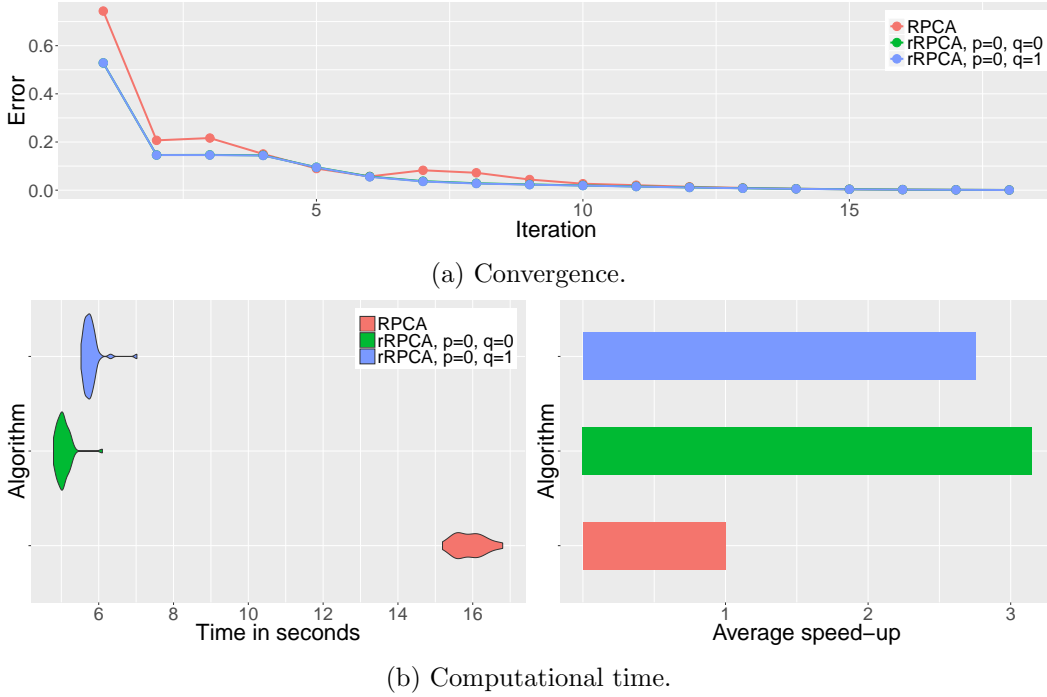


Figure 17: Subplot (a) shows the convergence rate of the robust PCA algorithm using both a deterministic and randomized SVD algorithm. Subplot (b) shows the corresponding computational times, indicating a speed-up factor of about 3.

#### 4.5. Computational performance.

The time complexity of classic deterministic SVD algorithms are  $O(mn^2)$ , where it is assumed that  $m \geq n$ . Modern partial SVD algorithms reduce the time complexity to  $O(mnk)$  (Demmel 1997). Randomized SVD, as presented here, comes also with asymptotic costs of  $O(mnk)$ . The key difference, however, is that the rSVD algorithm (without subspace iterations) requires only two passes over the input matrix. Hence, from a practical point of view, the algorithm is computationally more efficient.

Figure 18 shows the computational evaluation of the base `svd()` and `rsvd()` function on different random low-rank matrices. The computation time and the relative reconstruction errors are computed over a sequence of different target-ranks  $k$ . In particular, for very low-dimensional approximations, the achieved speed-up over the base `svd()` function is substantial, by a factor of about 5 to 150. The advantage of the randomized algorithm becomes pronounced with an increasing matrix dimension. The comparison of subplot (a) and (b) highlights the savings. Hence, the randomized SVD algorithm enables the decomposition of very large data matrices, where the standard algorithm is infeasible. Interestingly, the achieved speed-up for a tall and skinny matrix, as shown in subplot (c), is only significant for  $k \ll n$ . This is because the required QR-decomposition by the randomized algorithm is relatively expensive here. Overall, the reconstruction error with just  $q = 1$  subspace iteration is minor.

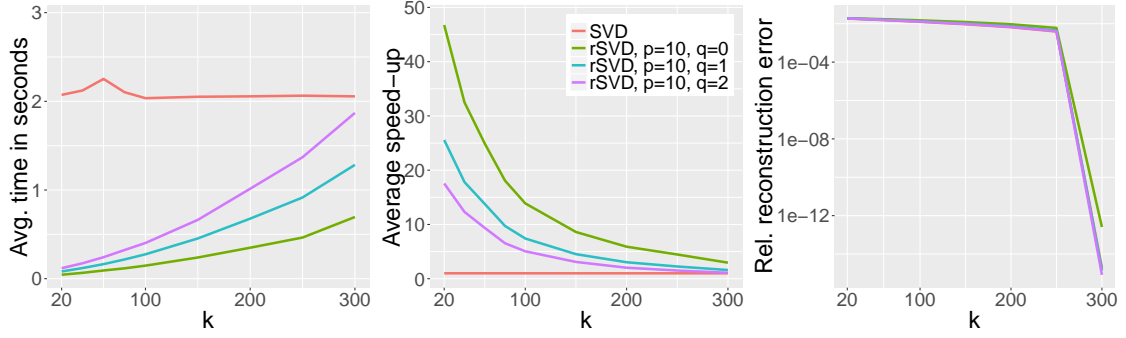
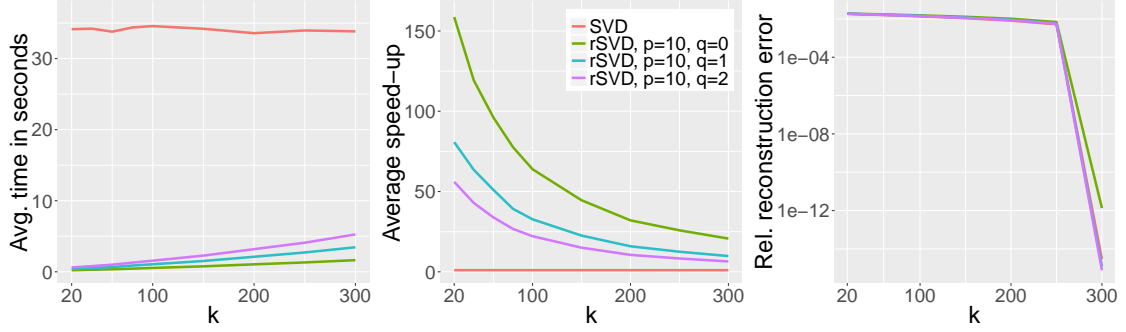
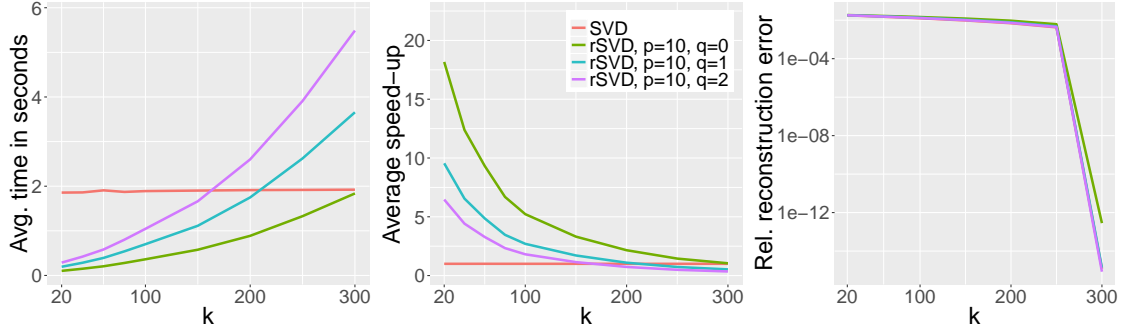
(a) Square (fat) matrix of size  $2000 \times 2000$ .(b) Square (fat) matrix of size  $5000 \times 5000$ .(c) Tall and skinny matrix of size  $10000 \times 1000$ .

Figure 18: Computational performance of the `rsvd()` function on three different random low-rank ( $r = 300$ ) matrices. The left column shows the average computational time and the middle column the achieved speed-up over the base `svd()` function. The right column shows the relative reconstruction error of the matrix approximation over varying target-ranks  $k$ .

## 5. Conclusion

Due to the tremendous increase of high-dimensional data produced by modern sensors and social networks, data methods for dimensionality reduction are becoming increasingly important. However, despite modern computer power, massive data-sets pose a tremendous computational challenge for traditional algorithms. Probabilistic algorithms can substantially ease the logistic and computational challenges in obtaining approximate matrix decompositions. This advantage becomes pronounced with an increasing matrix dimension. Moreover, randomized algorithms

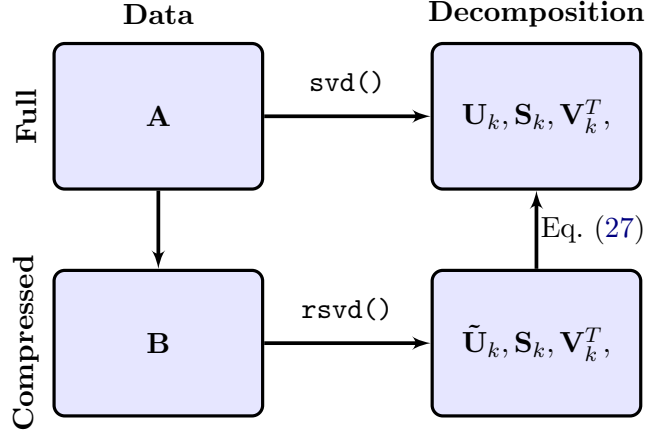


Figure 19: Conceptual architecture of the randomized singular value decomposition. The data are first compressed via right multiplication by a sampling matrix  $\Omega$ . Next, the SVD is computed on the compressed data. Finally, the left singular vectors  $\mathbf{U}_k$  may be reconstructed from the compressed singular vectors  $\tilde{\mathbf{U}}_k$  by the expression in Eq. (27).

are feasible for even massive matrices where traditional deterministic algorithms fail. The randomized singular value decomposition is the most prominent and ubiquitous randomized algorithm. Its popularity is due to the strong theoretical error bounds and the advantage that the error can be controlled by oversampling and subspace iterations. The concept is summarized in Figure 19.

The R package **rsvd** provides computational efficient randomized routines for the singular value decomposition, principal component analysis and robust principal component analysis. The routines are intuitive to use and the performance evaluation shows that the randomized algorithm provides an efficient framework to reduce the computational demands of the traditional (deterministic) algorithms. Specifically, speed-ups about 5 to 150 times are gained. Further, a feature of the implemented routines is that they provide the option to use either the randomized or deterministic algorithm.

The applications of the randomized matrix algorithms are ubiquitous and can be utilized for all methods relying on the computation of (generalized) eigenvalue problems. Future developments of the **rsvd** package will apply this concept to compute linear discriminant analysis, principal component regression, and canonical correlation analysis. Another important direction is to support a more efficient routine for massive sparse matrices. Moreover, randomized algorithms are embarrassingly parallel and can substantially benefit from a graphic processing unit (GPU) accelerated implementation.

## Acknowledgements

JNK acknowledges support from Air Force Office of Scientific Research (FA9500-15-C-0039). SLB acknowledges support from the Department of Energy (DE-EE0006785). NBE acknowledges support from the UK Engineering and Physical Sciences Research Council (EP/L505079/1).

## References

- Abdi H, Williams LJ (2010). “Principal component analysis.” *Wiley Interdisciplinary Reviews: Computational Statistics*, **2**(4), 433–459. doi:10.1002/wics.101.
- Anderson E (1935). “The Irises of the Gaspé Peninsula.” *Bulletin of the American Iris Society*, **59**, 2–5.
- Bouwman T, Sobral A, Javed S, Jung SK, Zahzah EH (2015). “Decomposition into Low-rank plus Additive Matrices for Background/Foreground Separation: A Review for a Comparative Evaluation with a Large-Scale Dataset.” *arXiv preprint arXiv:1511.01245*, pp. 1–121.
- Bouwman T, Zahzah EH (2014). “Robust PCA via Principal Component Pursuit: A Review for a Comparative Evaluation in Video Surveillance.” *Computer Vision and Image Understanding*, **122**, 22–34. doi:10.1016/j.cviu.2013.11.009.
- Candès EJ, Li X, Ma Y, Wright J (2011). “Robust Principal Component Analysis?” *Journal of the ACM (JACM)*, **58**(3), 11.
- Cohen MB, Lee YT, Musco C, Musco C, Peng R, Sidford A (2015). “Uniform Sampling for Matrix Approximation.” In *Proceedings of the 2015 Conference on Innovations in Theoretical Computer Science*, pp. 181–190. ACM.
- Cunningham JP, Ghahramani Z (2015). “Linear Dimensionality Reduction: Survey, Insights, and Generalizations.” *Journal of Machine Learning Research*, **16**, 2859–2900.
- Demmel J (1997). *Applied Numerical Linear Algebra*. Society for Industrial and Applied Mathematics. ISBN 9780898713893. doi:10.1137/1.9781611971446.
- Donoho DL (2000). “High-Dimensional Data Analysis: The Curses and Blessings of Dimensionality.” *AMS Math Challenges Lecture*, pp. 1–32.
- Eckart C, Young G (1936). “The Approximation of one Matrix by Another of Lower Rank.” *Psychometrika*, **1**(3), 211–218.
- Erichson NB, Donovan C (2016). “Randomized Low-Rank Dynamic Mode Decomposition for Motion Detection.” *Computer Vision and Image Understanding*, **46**, 40–50. doi:10.1016/j.cviu.2016.02.005.
- Fienup JR (1997). “Invariant Error Metrics for Image Reconstruction.” *Applied Optics*, **36**(32), 8352–8357.
- Frieze A, Kannan R, Vempala S (2004). “Fast Monte-Carlo Algorithms for Finding Low-Rank Approximations.” *Journal of the ACM*, **51**(6), 1025–1041.
- Gavish M, Donoho DL (2014). “The Optimal Hard Threshold for Singular Values is.” *Information Theory, IEEE Transactions on*, **60**(8), 5040–5053.
- Golub G, Kahan W (1965). “Calculating the Singular Values and Pseudo-Inverse of a Matrix.” *Journal of the Society for Industrial and Applied Mathematics, Series B: Numerical Analysis*, **2**(2), 205–224.



- Golub GH, Reinsch C (1970). “Singular Value Decomposition and Least Squares Solutions.” *Numerische Mathematik*, **14**(5), 403–420.
- Golub GH, Van Loan CF (1996). *Matrix Computations*. 3 edition. Johns Hopkins University Press, Baltimore, MD, USA. ISBN 0801854148.
- Goyette N, Jodoin PM, Porikli F, Konrad J, Ishwar P (2012). “Changedetection.net: A new change detection benchmark dataset.” In *Computer Vision and Pattern Recognition Workshops (CVPRW), 2012 IEEE Computer Society Conference on*, pp. 1–8. IEEE.
- Greenacre MJ (2010). *Biplots in Practice*. Fundacion BBVA.
- Gu M (2015). “Subspace Iteration Randomization and Singular Value Problems.” *SIAM Journal on Scientific Computing*, **37**(3), 1139–1173.
- Halko N, Martinsson PG, Shkolnisky Y, Tygert M (2011a). “An Algorithm for the Principal Component Analysis of Large Data Sets.” *SIAM Journal on Scientific Computing*, **33**(5), 2580–2594.
- Halko N, Martinsson PG, Tropp JA (2011b). “Finding Structure with Randomness: Probabilistic Algorithms for Constructing Approximate Matrix Decompositions.” *SIAM Review*, **53**(2), 217–288. doi:10.1137/090771806.
- Hastie T, Tibshirani R, Friedman J (2009). *The Elements of Statistical Learning: Data Mining, Inference, and Prediction*. Springer Series in Statistics, 2nd edition. Springer-Verlag. ISBN 9780387216065.
- Izenman AJ (2008). *Modern Multivariate Statistical Techniques: Regression, Classification, and Manifold Learning*. Springer-Verlag. ISBN 0387781889.
- Johnson WB, Lindenstrauss J (1984). “Extensions of Lipschitz Mappings into a Hilbert Space.” *Contemporary Mathematics*, **26**(1), 189–206.
- Jolliffe I (2002). *Principal Component Analysis*. Springer Series in Statistics, 2nd edition. Springer-Verlag. ISBN 9780387954424.
- Kirby M, Sirovich L (1990). “Application of the Karhunen-Loeve Procedure for the Characterization of Human Faces.” *Pattern Analysis and Machine Intelligence, IEEE Transactions on*, **12**(1), 103–108.
- Lin Z, Chen M, Ma Y (2010). “The Augmented Lagrange Multiplier Method for Exact Recovery of Corrupted Low-Rank Matrices.” *arXiv preprint arXiv:1009.5055*, pp. 1–23.
- Mahoney MW (2011). “Randomized Algorithms for Matrices and Data.” *Foundations and Trends in Machine Learning*, **3**(2), 123–224. doi:10.1561/22000000035.
- Martinsson PG, Rokhlin V, Tygert M (2011). “A Randomized Algorithm for the Decomposition of Matrices.” *Applied and Computational Harmonic Analysis*, **30**(1), 47–68. doi:10.1016/j.acha.2010.02.003.
- Martinsson PG, Voronin S (2015). “A randomized blocked algorithm for efficiently computing rank-revealing factorizations of matrices.” *ArXiv e-prints*. 1503.07157.

- Mersmann O, Beleites C, Hurling R, Friedman A (2015). *microbenchmark: Accurate Timing Functions*. R package version 1.4-2.1, URL <http://CRAN.R-project.org/package=microbenchmark>.
- Murphy KP (2012). *Machine Learning: A Probabilistic Perspective*. MIT Press. ISBN 9780262018029.
- Pearson K (1901). “On Lines and Planes of Closest Fit to Systems of Points in Space.” *Philosophical Magazine Series 6*, **2**(11), 559–572. doi:10.1080/14786440109462720.
- Rivasplata O (2012). “Subgaussian Random Variables: An Expository Note.” *Internet publication, PDF*. URL <http://www.stat.cmu.edu/~arinaldo/36788/subgaussians.pdf>.
- Rokhlin V, Szlam A, Tygert M (2009). “A Randomized Algorithm for Principal Component Analysis.” *SIAM Journal on Matrix Analysis and Applications*, **31**(3), 1100–1124.
- Sarlos T (2006). “Improved Approximation Algorithms for Large Matrices via Random Projections.” In *Foundations of Computer Science. 47th Annual IEEE Symposium on*, pp. 143–152.
- Soetaert K (2016). *plot3D: Plotting Multi-Dimensional Data*. R package version 1.1, URL <http://CRAN.R-project.org/package=plot3D>.
- Stewart GW (1993). “On the Early History of the Singular Value Decomposition.” *SIAM review*, **35**(4), 551–566.
- Szlam A, Kluger Y, Tygert M (2014). “An Implementation of a Randomized Algorithm for Principal Component Analysis.” *arXiv preprint arXiv:1412.3510*.
- Venables WN, Ripley BD (2002). *Modern Applied Statistics with S-PLUS*. Statistics and Computing. Springer-Verlag. ISBN 9780387954578. doi:10.1007/978-0-387-21706-2.
- Voronin S, Martinsson PG (2015). “RSVDPACK: Subroutines for Computing Partial Singular Value Decompositions via Randomized Sampling on Single Core, Multi Core, and GPU Architectures.” *arXiv preprint arXiv:1502.05366*, pp. 1–15.
- Watkins DS (2002). *Fundamentals of Matrix Computations*. 2 edition. John Wiley & Sons. ISBN 9780470528334. doi:10.1002/0471249718.
- Wickham H (2009). *ggplot2: Elegant Graphics for Data Analysis*. Springer-Verlag. ISBN 9780387981406. URL <http://had.co.nz/ggplot2/book>.
- Woolfe F, Liberty E, Rokhlin V, Tygert M (2008). “A Fast Randomized Algorithm for the Approximation of Matrices.” *Applied and Computational Harmonic Analysis*, **25**(3), 335–366.
- Wright J, Ganesh A, Rao S, Peng Y, Ma Y (2009). “Robust Principal Component Analysis: Exact Recovery of Corrupted Low-Rank Matrices via Convex Optimization.” In *Advances in Neural Information Processing Systems*, pp. 2080–2088.
- Yu S, Tranchevent L, Moreau Y (2011). *Kernel-Based Data Fusion for Machine Learning: Methods and Applications in Bioinformatics and Text Mining*. Studies in Computational Intelligence. Springer-Verlag. ISBN 9783642194054.

**Affiliation:**

N. Benjamin Erichson  
School of Mathematics and Statistics  
University of St Andrews  
St Andrews, UK  
E-mail: [nbe@st-andrews.ac.uk](mailto:nbe@st-andrews.ac.uk)

Sergey Voronin  
Department of Mathematics  
Tufts University  
Medford, Massachusetts, U.S.

Steven L. Brunton  
Department of Mechanical Engineering  
University of Washington  
Seattle, Washington, U.S.

J. Nathan Kutz  
Department of Applied Mathematics  
University of Washington  
Seattle, Washington, U.S.